UNIVERSITY OF THE FREE STATE
UNIVERSITEIT VAN DIE VRYSTAAT
YUNIVESITHI YA FREISTATA

UFS HEALTH SCIENCES

IN VITRO EVALUATION OF EXPRESSION LEVELS OF ABC-TRANSPORTER GENES ON NEEDLE BIOPSIES OF PROSTATE CANCER PATIENTS TREATED WITH CHEMOTHERAPY

Submitted in fulfillment of the requirements in respect of the master's degree:

MASTER OF MEDICAL SCIENCE (M. Med.Sc) IN PHARMACOLOGY

By: Nandi Ngesi

Student number: 2010031975

B.Sc. (Biochemistry), B. Med.Sc Hons (Pharmacology)

Faculty of Health Sciences

Department of Pharmacology

University of the Free State

Supervisor: Prof. MP Sekhoacha

Co-Supervisor: Dr. BR Abrahams

29 November 2023

Abstract

Introduction: Prostate cancer (PCa) is the second-most diagnosed cancer among men worldwide, and the foremost male malignancy in South Africa. Various therapies are used in the treatment of PCa patients. However, despite advances in cancer therapy, treatment failures still lead to the advancement of the disease, relapse, and ultimately mortality. Chemotherapy is the treatment of choice for metastatic PCa, but it is challenged by multidrug resistance (MDR) of cancer cells. Various mechanisms participate in the MDR of cancer cells, including an increase in drug efflux facilitated by members of the ATP-binding cassette (ABC) transporters such as ATP-binding cassette sub-family C (ABCC1) / multidrug resistance-associated protein (MRP1), ABCC2/MRP2, and ABCC10/MRP7. Therefore, discovering drug resistance biomarkers and mechanisms is essential in both understanding and combating chemoresistance. This study identifies cellular drug transporter genes (ABCC1, ABCC2, and ABCC10) as possible targets for the prediction of docetaxel treatment outcomes in PCa patients.

Purpose: The aim of this study was to investigate whether a correlation exists between the expression levels of ABCC1, ABCC2, and ABCC10 transporter genes and good versus (vs) poor responses to chemotherapy.

Methods: A total of nine Formalin-Fixed Paraffin-Embedded (FFPE) tissue biopsies of PCa patients were obtained from National Health Laboratory Service, Universitas academic hospital, and divided into two categories, good and poor responders. RNA and proteins were extracted from the FFPE tissues, quantified, and evaluated using quantitative RT-PCR and western blot.

Results: quantitative RT-PCR shows that ABCC1/MRP1, ABCC2/MRP2, and ABCC10/MRP7 were expressed in the good and poor responder categories of PCa patients. In the good responder category, 50 % of the patients showed elevated expression levels of ABCC1/MRP1 and ABCC10/MRP7 in the normal sections compared to their tumour sections. The expression level of ABCC2/MRP2 was elevated in 75 % of the patients' normal sections in comparison to their tumour sections. Moreover, in the

poor responder category, 80 % of the patients showed elevated expression of ABCC1 in the tumour sections compared to the normal sections, and 60 % of patients showed elevated expression levels of ABCC10 in the tumour sections compared to their normal sections. The expression levels of ABCC2 in the tumour and normal sections of patients in this category of poor responders, could not be compared because the expression levels of ABCC2 could not be determined in 50 % of the patient samples. The average expression levels of ABCC1 and ABCC10 were upregulated in the tumour sections of patients in the poor responder category but were deregulated in the tumour sections of patients in the good responder category. Additionally, ABCC1, ABCC2, and ABCC10's average expression levels were upregulated in the normal sections of patients in the good responder category and deregulated in the normal sections of patients in the poor responder category.

Conclusions: The results suggest that a correlation exists between the expression levels of ABCC1, ABCC2, and ABCC10 and drug resistance reported in the poor responder category. Also, the detection of these transporter genes could potentially be used as indicators of possible docetaxel treatment outcomes.

Keywords: prostate cancer, chemoresistance, docetaxel, ABC-transporters, FFPE tissue, RNA extraction, protein extraction, quantitative RT-PCR, protein staining, western blot

Declaration of independent work

I, Nandi Dinah Ngesi, hereby declare that the dissertation entitled: *In vitro* evaluation of expression levels of ABC-transporter genes on needle biopsies of prostate cancer patients treated with chemotherapy, hereby submitted by me for M.Med.Sc. master's degree in pharmacology at the University of the Free State is my own independent work and has not previously been submitted by me at another university or faculty for admission to a degree or diploma. I furthermore cede copyright of the dissertation to the University of the Free State.

Date ……12 February……. Signature ……

Supervisor's declaration:

I, Professor Mamello Patience Sekhoacha, the supervisor of the master's research dissertation entitled: *In vitro* evaluation of expression levels of ABC-transporter genes on needle biopsies of prostate cancer patients treated with chemotherapy, hereby certify that the work in this project was done by Nandi Dinah Ngesi at the Department of Pharmacology, University of the Free State. I hereby approve the submission of this thesis and also affirm that this has not been submitted previously, either in part or in its entirety, to the assessors, neither to this or any other institution for admission to a degree or any other qualification.

Date ……12 February 2024…… Signature ……

Acknowledgements

The following individuals deserve recognition and gratitude for their significant contributions to the completion of this thesis:

- To the all-powerful God who has given me wisdom, comprehension, strength, and fortitude to carry out this project until completion.
- My sincere gratitude goes out to my supervisor, Prof. Mamello Sekhoacha, for all her assistance, understanding, encouragement, and support during this journey. I'm grateful that you were there for me during a particularly trying period. I also appreciate the opportunities of growth you awarded me.
- To my co-supervisor, Dr. Abrahams, thank you for your technical support and scientific input. You always went above the call of duty to assist with practical work and providing the required resources.
- Administratively, I would like to acknowledge the National Research Foundation Thuthuka grant, for their financial support during this masters' programme.
- I am grateful to the NHLS for approving this study and supplying the archived biological materials used in this research project.
- Above all, I want to express my gratitude to my family, Bongani Ngesi, Ntambose Mabaso, and Ntethekazi Mokoena, for their prayers, unconditional love, steadfast support, and constant encouragement. I couldn't have made it through the most challenging of times without you. You are special!

Table of Contents

List of Abbreviations

%	Percentage
≤	Less than or equal to
µg/ml	Microgram per milliliter
µl	Microliter
µg/L	microgram per litre
^{0}C	Degrees celsius
AARMS	Academic affairs and research management system
ABC	Adenosine triphosphate binding cassette
ABC	ATP-binding cassette
ABCB1	Adenosine triphosphate binding Cassette Subfamily B Member 1
ABCC1	Adenosine triphosphate binding cassette subfamily C member 1
ABCC10	Adenosine triphosphate binding cassette subfamily C member 10
ABCC2	Adenosine triphosphate binding cassette subfamily C member 2
ABCG2	Adenosine triphosphate binding cassette subfamily G member 2
ADT	Androgen deprivation therapy
AIPC	Androgen-independent prostate cancer
AJCC	American joint committee on cancer
Amplicon	PCR Product
AR	Androgen Receptor
ATP	Adenosine triphosphate
BCA	Bicinchoninic acid
BCRP	Breast cancer resistance protein
bp	Base pairs
BSA	Bovine serum albumin
cc	cubic centimetre
cm	centimetres
cMOAT	Canalicular multiple organic anion transporter
Cq	Quantification cycle

CT	Threshold cycle
Cu^{1+}	Cuprous ions
CYP3A4	Cytochrome P450 3A4
CYP3A5	Cytochrome P450 3A5
DNA	Deoxyribonucleic acid
DRE	Digital rectal examination
DU145	Human prostate cancer cell line
DV200	Percentage of RNA fragments with a length >200 nucleotides
$E_2$17βG	Estradiol glucuronide
EBRT	External beam radiation therapy
EGFR	Epidermal growth factor receptor
EMT	Epithelial mesenchymal transition
Erk	Extracellular signal-regulated kinase
FDA	Food and drug administration
FFPE	Formalin fixed paraffin embedded
g	gram(s)
GAPDH	Glyceraldehyde-3-phosphate dehydrogenase
GR	Good responder
GS	Gleason score
HCl	Hydrochloric acid
HDR	High-dose-rate
HepG2	Hepatocellular carcinoma
HPRT	Hypoxanthine-guanine phosphoribosyltransferase
hr.	Hour
HRPC	Hormone-refractory prostate cancer
HSP	Heat shock protein
HSP27	Heat shock protein 27
HSP90	Heat shock protein 90
HSPCB	Heat shock protein calmodulin binding gene
kDA	Kilodalton
LDR	Low-dose-rate

LTC4	Leukotriene C4
mCRPC	Metastatic castration resistant prostate cancer
mCSPC	Metastatic castration sensitive prostate cancer
MDR	Multidrug resistance
MDR1	Multidrug resistance 1/ P-glycoprotein
mg/ml	Milligram per milliliter
MIQE	Minimum Information for publication of quantitative real-time PCR Experiments
ml	Mililiter
MRI	Magnetic resonance imaging
mRNA	Messenger Ribonucleic acid
MRP1	Multidrug resistance protein 1
MRP2	Multidrug resistance protein 2
MRP7	Multidrug resistance protein 7
MSD	Membrane-spanning domain
N	Normal
NBD	Nucleotide binding domains
NCBI	National centre for Biotechnology Information
NF-κB	Nuclear factor
ng	Nanogram
ng/µL	Nanogram per microliter
ng/ml	nanogram per millilitre
NHLS	National health laboratory service
nm	Nanometer
NRT	No reverse transcriptase control
NSCLC	Non-small cell lung cancer
NTC	No template control
PBS	Phosphate-buffered Saline
PC3	Prostatic cell carcinoma
PCa	Prostate cancer
PCR	Polymerase chain reaction
PI3K	Phosphoinositide 3-kinase

PR	Poor responder
PSA	Proste-specific antigen
qPCR	Quantitative polymerase chain reaction
qRT-PCR	Quantitative real-time polymerase chain reaction
RIN	RNA Integrity Number
RNA	Ribonucleic acid
RT	Reverse Transcriptase
s	Seconds
SDS	Sodium dodecyl sulfate
T	Tumour
Ta	Annealing temperature
Tm	Melting temperature
TM	transmembrane
TMD	Transmembrane domains
TNM	Tumour, Node, Metastasis
TRUS	Transrectal ultrasound scan
vs.	Versus
w/v	Weight in volume

List of Figures

List of Tables

CHAPTER 1:

INTRODUCTION

1.1 Introduction

Prostate cancer (PCa) is the second-most diagnosed cancer among men worldwide, and the foremost male malignancy in South Africa (Sánchez et al., 2009, Cassim et al., 2021). Prostate cancer is a condition where cancer cells develop in the prostate tissue. The prostate is a walnut-shaped gland at the base of the male bladder that contributes to the seminal fluid that nurtures and carries sperm (Harvard Health Medical Dictionary, accessed 24 January 2024). PCa can be detected during a routine digital rectal examination (DRE); prostate-specific antigen (PSA) testing; and transrectal ultrasound scan (TRUS) and transrectal magnetic resonance imaging (MRI). Subsequently, diagnosis is made when the cancerous cells are recognized in prostate tissue obtained through a needle biopsy (National Cancer Institute, accessed 17 August 2021). Following diagnosis, the oncologist prescribes a treatment plan for the patient based on the PSA level, grade group, age, stage and other medical conditions of the patient (Draisma et al., 2006, Zheng et al., 2020). Currently, various treatments are being employed to treat PCa patients. These include active surveillance; radiation therapy; surgery; hormone therapy; chemotherapy; cryotherapy; and immunotherapy (National Cancer Institute, accessed 17 August 2021).

Despite advances in cancer therapy, treatment failures still lead to the advance of the disease, relapse and ultimately mortality (Begicevic and Falasca, 2017). Chemotherapy is the treatment of choice for metastatic prostate cancer. Chemotherapy is, however, challenged by multidrug resistance (MDR) of cancer cells, especially in the therapy of metastatic cancers, a phenomenon known as chemoresistance. Chemoresistance in patients can be divided into two classes: intrinsic resistance and acquired resistance. Intrinsic resistance is affiliated with the genetic traits of the tumour cells which serve as a defense mechanism for survival; whereas acquired resistance is because of exposure of tumour cells to the chemotherapeutic agents, at concentrations that are below therapeutic

doses (Kachalaki et al., 2016). Different mechanisms are associated with MDR, these include decreased uptake of water-soluble drugs; promotion of DNA damage repair; suppression of cell programmed death; increase in drug efflux; and alteration of the drug metabolism and cell cycle. Of all these drug resistance mechanisms, an increase in drug efflux is the most common, and most extensively studied, mechanism (Kachalaki et al., 2016, Hasan et al., 2018).

Increased drug efflux is often caused by the elevated outflow of chemo drugs by cell membrane transporters, which leads to reduced intracellular concentrations of anticancer drugs, and a resultant reduction in the efficacy of the drugs (Choi, 2005, Sone et al., 2019). Drug transporters that belong to the ATP-binding cassette (ABC) transporter superfamily play a vital role in MDR. These transporters have clinical significance in influencing treatment outcomes of cancer patients. Thus far, 49 different ABC transporter genes have been identified and divided into seven classes (Kachalaki et al., 2016, Domenichini et al., 2019). Of the 49 ABC transporters, the most-researched members are ABCB1 (named MDR1 or P-glycoprotein), ABCC1 (multidrug resistance-associated protein, MRP1) and ABCG2 (breast cancer resistance protein, BCRP). These three multidrug transporters function as efflux pumps, and are highly expressed in most drug-resistant tumours, and account for most cases of chemoresistance (Begicevic and Falasca, 2017).

This study investigated the impact of ABCC1, ABCC2 and ABCC10 transporter genes (associated proteins are MRP1, MRP2 and MRP7, respectively) on drug resistance in clinical prostate cancer. The selection of the three genes was based on their transportation of various chemo drugs, including docetaxel. The study focusses on the correlation between the expression levels of these genes and the treatment outcome of PCa patients treated with docetaxel. The study specimens (needle biopsies) were collected retrospectively from PCa patients in the period of January 2015 to January 2022 and archived at the National Health Laboratory Service (NHLS) at Universitas Academic Hospital in Bloemfontein, Free State. The sample size was ten specimens (n=10), divided into two categories, five good responders (sensitive to docetaxel) and five poor responders (resistant to docetaxel), based on the anonymized clinical data obtained from

the oncologist, and pertaining to the treatment outcomes of patients treated with docetaxel.

This pilot study employs mainly *in vitro* bioassays and genetic evaluation to investigate the impact of expression levels of those genes at a proteomic and genetic level, using retrospect biological material and associated data (outlining the treatment response of the patients) stored at the department of anatomical pathology of the National Health Laboratory Service.

The overall value of the study is to serve as proof of concept for pharmacogenetics, which encompasses studying the effects of the expression of certain target genes to drug response. The study could ultimately link to a bigger pharmacogenomic study, which entails studying individual differences in drug response in relation to their genetic profile. The concept of pharmacogenetics in PCa, has not been extensively explored in South Africa. It is envisaged that this study, although at a pilot scale for proof of concept, will contribute to the body of knowledge on molecular biomarker research, the suitability of methods used, and the predictability of treatment outcomes in PCa patients treated with docetaxel in South Africa. The study identifies cellular drug transporter genes (ABCC1, ABCC2 and ABCC10) as possible targets for prediction of treatment outcomes in PCa patients. The prediction of treatment outcome would ultimately influence the prescription of the treatment regime in terms of doses and additional drugs that can be co-administered to maximize effectiveness.

1.2 Problem Statement

PCa is one of the most prevalent male malignancies in the world, and is responsible for a substantial number of cancer-related mortalities (Bergengren et al., 2023). Mortality is primarily due to disease advancement as observed in metastatic castration resistant PCa (mCRPC). Various anticancer drugs have been explored in mCRPC. However, docetaxel, was the initial treatment that significantly improved the survival rate (Lima et al., 2021). Docetaxel remains commonly used as a first-line treatment of mCRPC. The study conducted by Parker et al (2015) reflected that although the survival improvement observed in mCRPC patients was two-to-three months, it was substantial (Lima et al.,

2021). Unfortunately, patients inevitably succumb to the advancement of the disease due to acquired drug resistance. Even though the mechanisms by which PCa acquire resistance to docetaxel remain unclear, earlier studies have reported several resistance mechanisms including increased drug efflux, facilitated by ABC-transporters, such as MRP1 (ABCC1), MRP2 (ABCC2), and MRP7 (ABCC10), among others (Lima et al., 2021).

Understanding the involvement and impact of ABC-transporters on treatment outcome would facilitate two significant objectives: Before drug treatment, patients who will not respond to chemotherapy could be identified, minimizing unnecessary toxicity, and permitting them to move to alternate forms of treatment. Secondly, there may also be opportunities to explore new therapeutic targets (Mahon et al., 2011). The goal is to recognize patients who are resistant to treatment and provide them an alternate course of action (Rodrigues-Ferreira et al., 2021). Furthermore, evaluating the heterogeneity of patients with the same condition, and chemotherapy resistance, has led to substantial therapy in personalized medicine. Therefore, discovering drug resistance biomarkers and mechanisms is essential in order to personalize treatment and enhance survival (Mahon et al., 2011).

1.3 Study Rationale

Cancer biomarkers are generated by malignant cells, or normal cells, in reaction to cancer and are present in tissues or body fluids. Biomarker testing in cancer entails analyzing bodily fluids or tumours to identify modifications in proteins, DNA, RNA, or other biological molecules that offer information for cancer detection, outcomes, precision therapy, or predicting response to drugs (Sarhadi and Armengol, 2022). Consequently, biomarkers are becoming more important in improving cancer treatment outcomes. Predictive biomarkers in particular are being used in precision therapy as certain tumour modifications or variations in genes (pharmacogenetics) result in a specific pattern of sensitivity to chemotherapeutic agents (Sarhadi and Armengol, 2022).

The aim of predictive biomarkers is to estimate the result of a specific treatment on a cancer patient before commencement of therapy. Based on the results of biomarker

testing, cancer patients can be grouped as probable non-responders, responders, or exhibiting toxicity to a specific treatment. In individuals deemed as non-responders or at risk of toxicity, predictive biomarkers can be helpful in suggesting alternative therapy or modifying treatment dosages (Sarhadi and Armengol, 2022).

The current study investigated the expression of ABC-transporter genes (ABCC1, ABCC2, ABCC10) as potential predictive biomarkers in PCa patients treated with docetaxel. This concept could be employed in the future as a diagnostic tool, to determine docetaxel treatment prognosis in PCa patients identified to undergo treatment. The information generated from this study could potentially be used to guide medical professionals on treatment regime selection and dosages that are most appropriate for South African PCa patients.

1.4 Research Questions

The main research questions of this study were the following:

1. How does the expression of ABC-transporter genes (ABCC1, ABCC2, ABCC10) impact good versus poor treatment outcomes in PCa patients treated with docetaxel?

2. Can ABCC1, ABCC2, and ABCC10 transporter genes be utilized as biomarkers to predict treatment outcomes in PCa patients?

1.5 Aim

Investigate whether a correlation exists between the expression levels of ABCC1/MRP1, ABCC2/MRP2, and ABCC10/MRP7 transporter genes and poor versus good response to chemotherapy in PCa patients.

1.6 Objectives

1.6.1 Obtain FFPE tissue biopsies of prostate cancer patients and categorize those biopsies according to the patients' responses to treatment: good responders (chemo sensitive) versus poor responders (chemo resistant) to chemotherapy using docetaxel.

1.6.2 Extract and quantify total RNA and proteins from the categorized groups of FFPE tissues.

1.6.3 Evaluate the expression of ABCC1, ABCC2, and ABCC10 transporter target genes through quantitative RT-PCR and the expression of their associated proteins (MRP1, MRP2 and MRP7) respectively, through western blot, by using the extracted RNA and proteins.

1.6.4 Determine whether a correlation exists between ABCC1, ABCC2, and ABCC10 expression levels and drug resistance experienced by patients, from the biopsies that were obtained.

1.6.5 Determine whether the detection of transporter genes ABCC1, ABCC2, and ABCC10 can be used as indicators of possible treatment responses.

CHAPTER 2:

LITERATURE REVIEW

2.1 The Prostate Anatomy

The human prostate gland is a pyramid-shaped organ positioned behind the bladder, with the peak contacting the penile urethra and the base contacting the bladder. The prostate is placed in front of the rectum, just below the urinary bladder. The prostate surrounds the prostatic urethra, which transports urine from the bladder (Ittmann, 2018). It is essential for partly producing the fluid that is part of the semen. Following puberty, the prostate gland grows because of the spike in testosterone. In a typical adult, it grows to a size of 20 cc and is 3 cm long, 4 cm wide, and 2 cm deep. Its dimensions and form can be compared to those of a walnut (Sooriakumaran et al., 2012)

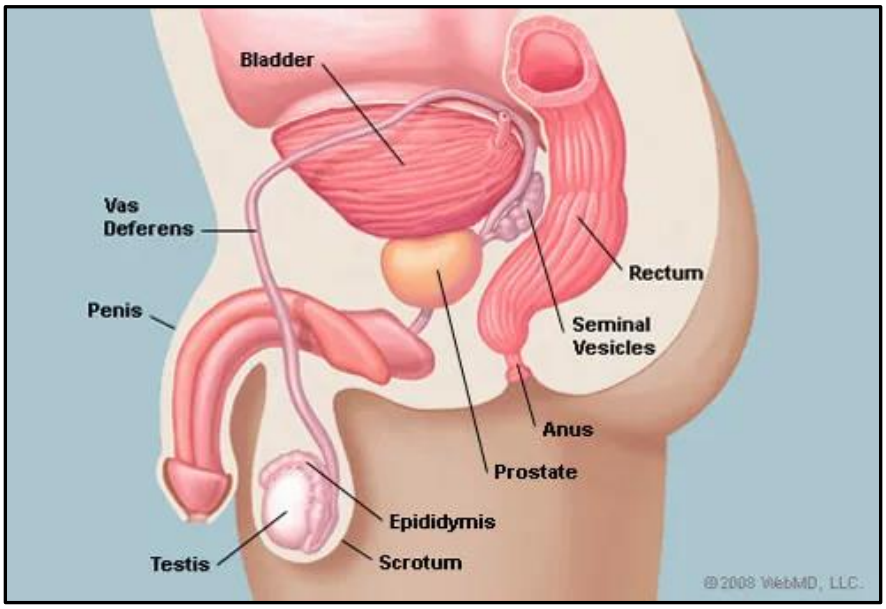

Figure 1: The male anatomy (emedicinehealth, accessed 03 October 2023).

Furthermore, the prostate gland has an inverted cone form and weighs 30-40 g in an adult whose prostatic hyperplasia is not severe. Because is anterior to the rectum, with the urethra running across its middle, it acts as a crucial point for comparison. As a result,

transrectal needle biopsy and transurethral excision are both feasible procedures for the prostate (Shah and Zhou, 2019).

In terms of its anatomy, it is made up of three zones, namely: the peripheral, central and transition zones. Each of these zones has a distinct histology, disease preference, and volume. Table 1 and Figure 2 below, presents the three different zones of the prostate gland (Shah and Zhou, 2019).

Table 1: Anatomy, disease preference and sampling techniques of the three zones of the prostate (Shah and Zhou, 2019).

	Peripheral Zone	Central Zone	Transition Zone
Anatomical Landmarks			
Location inside the prostate	Horseshoe shaped zone that borders the central zone closely and the end of the prostatic urethra distally on the posterior side.	Inverted cone-shaped area that borders the ejaculatory tubes. Its base is at the bladder neck and top at the seminal colliculus.	The proximal prostatic urethra's anterior side.
Disease Preference			
Atrophy	Regular	Irregular	Fluctuates
Non-cancerous Prostate enlargement	Irregular	Rare	Regular
Inflammation	Regular	Irregular	Fluctuates
Carcinoma (% of total cancer)	70%	10%	20%
Methods for tissue sampling			
Transrectal-needle biopsy	Good	Good	Poor
Transperineal needle biopsy	Good	Good	Good
Transurethral resection	Poor	Poor	Good

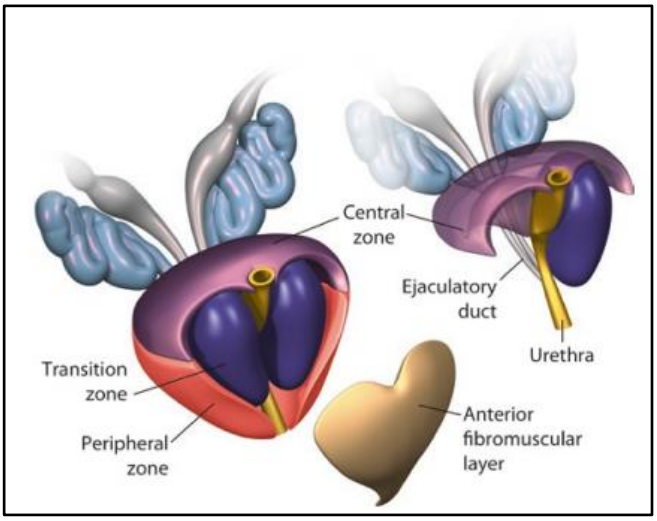

Figure 2: Graphical illustration of the three zones of the prostate gland (Shah and Zhou, 2019).

2.2 Prostate Cancer

The development of PCa is initiated when the prostate gland cells multiply uncontrollably (American Cancer Society, accessed 31 May 2021). PCa is a heterogenous disease with genetic and environmental factors affecting the onset and course of the disease. Most PCas are of prostatic glandular origin, i.e., adenocarcinoma, although occasionally other forms of cancer, such as urothelial (transitional cell) carcinoma and small cell carcinoma, may develop within the prostate. The absence of a basal cell layer, nuclear expansion, and conspicuous nucleoli, are the three most significant cytological characteristics of PCa (Sooriakumaran et al., 2012). There are risk factors which contribute to the development of PCa. To target primary and secondary prevention, it is essential to identify and understand them (Bergengren et al., 2023).

2.2.1 Risk factors

The well-established nonmodifiable risk factors for PCa are race, family history, germline mutations, and age. The modifiable risk factors, on the other hand, include metabolic syndrome, smoking, and obesity. Further multitude of risk factors related to infection, food, lifestyle, and environment, may contribute to the genesis of PCa. However, the evidence for this is rather limited (Bergengren et al., 2023). In this study, emphasis is placed on age, because it is a risk factor that is observed in the patient population selected for the study.

Age is one of the biggest risk factors for prostate cancer development (William et al., 2012, Rawla, 2019). Ageing has been linked to a series of ongoing physiological changes that include tissue hypoxia, immune system suppression (also known as immunosenescence), variations in hormone levels, and modifications to DNA repair pathways (William et al., 2012). Additionally, linked to aging are changes in repair mechanisms and DNA mutations that raise the risk of cancer. Prostate cancer has been demonstrated to have mitochondrial DNA damage, which is aggravated by reactive oxygen species and a deficiency in repair (William et al., 2012, Bernstein et al., 2013).

PCa is detected in a minority of people younger than 50 years, which is less than 0.1 % of all patients. The average age of patients with this condition is 72-74 years, and around 85 % of patients are diagnosed after 65 years. At 85 years, the growing risk of PCa varies from 0.5 % to 20 % worldwide. Data collected from autopsy studies suggest that most men older than 85 years have histological PCa (Grönberg, 2003). According to recent US cancer data, the lifetime likelihood of prostate cancer (PCa) is 12.5 %, with an increase in probability from 1.8 % in men aged 60–69, to 9.0 % in men aged 70 and above. Autopsy studies report that 40 % of unscreened males over 60 years old have PCa; this number rises to 60 % in men over 80 years old (Bergengren et al., 2023).

2.2.2 Prostate cancer statistics

Prostate cancer is the second-most common cancer and was the fifth-most common cause of cancer-related mortality for males, globally, in 2020, with an expected 1.4 million new cases and 375,000 deaths from the disease. While death rates are less varied (8.1 and 5.9 per 100,000, respectively), incidence rates are three times greater in developed than in developing nations (37.5 and 11.3 per 100,000, respectively) (Rawla, 2019, Sung et al., 2021). It is the most common type of cancer diagnosed in men in more than half (112 of 185) of the world's nations. Geographically, incidence rates range from 6.3 to 83.4 per 100,000 men: northern and western Europe, the Caribbean, Australia/New Zealand, north America, and southern Africa have the greatest rates, while Asia and northern Europe have the lowest rates (Sung et al., 2021).

When compared to people in sub-Saharan Africa and lower-income countries, research indicates that prostate cancer rates are rather high in South Africa. Prostate specific antigen (PSA) screening for prostate cancer is not part of any national programme in South Africa. In addition, there is no organized national campaign to educate the public about prostate cancer (Gray et al., 2020).

Table 2, below, shows the approximate number of new cases and deaths reported globally, in 2020, for PCa. It is believed that there is an underestimation of PCa in Africa, as there might be an elevated level of under-diagnosis as a result of poor access to testing and diagnostic facilities (Babb et al., 2014). The reported number of PCa deaths in

Southern Africa in Table 2, for males in the age group of 40 – 84 years is 13 450 and 3978 respectively. This study focuses on the treatment outcome of prostate cancer patients between the ages of 40 – 80 years, which is the target group for the current study. A rapid diagnosis and application of new and relevant chemotherapeutic treatment regimens could potentially improve the prognosis of patients, halt cancer progression and ultimately reduce the mortality rates of PCa patients in Southern Africa.

Table 2: Approximated number of new cases and death, globally, in 2020, for PCa, in men between the ages of 40 and 84 years (Globocan, accessed 03 October 2023).

	New Prostate Cancer cases in 2020 (Age 40-84)				Prostate Cancer deaths in 2020 (Age 40-84)			
Population	Number	Crude Rate	ASR (World)	Cum. Risk (%)	Number	Crude Rate	ASR (World)	Cum. Risk (%)
Eastern Asia	223 060	55.6	47.9	4.87	53 516	13.3	10.8	1.55
Northern America	232 589	281.7	227.5	13.50	28 026	37.2	32.0	4.17
Western Europe	158 399	323.2	237.3	16.08	25 680	31.1	19.7	2.42
South America	146 206	194.1	186.1	14.07	29 757	46.8	36.7	4.04
Central and Eastern Europe	106 750	167.8	140.8	10.97	20 072	41.0	21.8	2.84
Southern Europe	92 664	228.8	182.5	11.92	22 873	7.5	8.0	0.88
Northern Europe	86 301	344.5	252.6	17.44	13 183	52.6	28.3	3.85
South-Central Asia	49 474	16.2	17.4	1.70	12 712	31.4	17.5	2.31
South-Eastern Asia	38 198	34.1	38.0	3.58	12 385	11.0	12.0	1.68
Central America	33 281	126.4	128.4	10.22	14 316	41.1	54.8	5.52
Western Asia	28 944	67.0	83.5	7.37	12 308	33.7	44.8	4.80
Western Africa	25 740	73.9	95.4	7.99	7 543	28.6	26.4	3.40
Eastern Africa	22 494	61.6	80.9	7.29	6 923	89.1	65.9	8.62
Caribbean	19 681	253.2	226.2	15.78	7 066	16.4	19.3	2.78
Australia and New Zealand	19 910	298.9	233.9	15.19	7 178	49.9	65.7	7.11
Northern Africa	14 341	43.1	45.5	4.82	4 803	14.4	14.1	2.74
Southern Africa	13 450	155.0	189.2	15.54	3 978	45.9	57.8	6.45
Middle Africa	12 808	89.1	116.1	10.41	2 572	38.6	22.1	3.04
Melanesia	1 142	84.9	106.0	8.12	407	30.3	41.6	5.67
Polynesia	213	188.8	191.4	15.82	60	53.2	51.6	6.11
Micronesia	100	117.0	121.5	10.65	28	32.8	35.1	4.81

2.3 Prostate cancer diagnosis:

Prostate cancer can be detected through PSA testing, a routine DRE, and diagnosis can be confirmed through a tissue biopsy of the prostate gland (National Cancer Institute, accessed 17 August 2021). Each of these techniques is explored in detail below.

2.3.1 Prostate-specific antigen (PSA)

PSA is an enzyme that takes the form of a 237 amino acid glycoprotein and is largely made by prostate gland cells that line the acini and ducts. Its primary biological role is to dissolve the proteins that cause the newly ejaculated semen to gel. PSA is also present at basal levels in men's normal serum, but is frequently raised in PCa (Prasanna Sooriakumaran and Tewari, 2012). PSA can also be increased by other disorders such as inflammation, trauma caused by urinary catheterization, benign prostate hyperplasia, and urinary tract infection, and is not particular to PCa (Weston et al., 2012).

Age-stratified diagnostic PSA levels are utilized: In men 50-59 years, a PSA cut-off of 3 µg/L is used to suggest the existence of PCa, whereas in older men, PSA values of >3 µg/L are needed to raise suspicion for PCa. However, elevated PSA levels do not always correlate with age and are not always an indicator of PCa. Therefore, on their own, they are not a reliable diagnostic tool (Muazzam et al., 2023). Cases of PCa with PSA levels <4 ng/mL have led to inaccurate findings and missed diagnoses. As a result, there is no consistent PSA range that can be used to clearly identify the existence of PCa in the early stage of the illness (Muazzam et al., 2023).

2.3.2 Digital rectal examination (DRE)

PCa typically develops on the gland's periphery, and diagnosis is possible even in its early stages of development, using a DRE. The doctor may feel a solid nodule inside the prostate gland in localized illness, where the cancer is restricted to the organ (Weston et al., 2012). When the gland feels particularly odd and has an atypical shape or deformed structure, it frequently indicates that the disease has progressed locally. Before being able to accurately detect an aberrant or worrisome gland, the physician must undertake numerous examinations to understand typical prostatic variation, just like with any other examination skill (Weston et al., 2012).

Screening with a digital rectal examination (DRE), prostate-specific antigen (PSA) test, or both has become standard clinical practice (Naji et al., 2018). DRE is valuable in the diagnosis of PCa and complements PSA and imaging (Weston et al., 2012). When combined with other indicators like PSA, DRE significantly enhances prostate cancer risk assessment (Walsh et al., 2014). People with a normal PSA may have PCa, either in the case of an advanced, poorly differentiated, non-PSA-secreting PCa, or in early small volume but palpable disease, both of which could be easily missed without a DRE. Additionally, once the diagnosis of PCa has been made, transrectal ultra-sonography or MRI are typically employed, but only to localize samples or stage the disease (Weston et al., 2012).

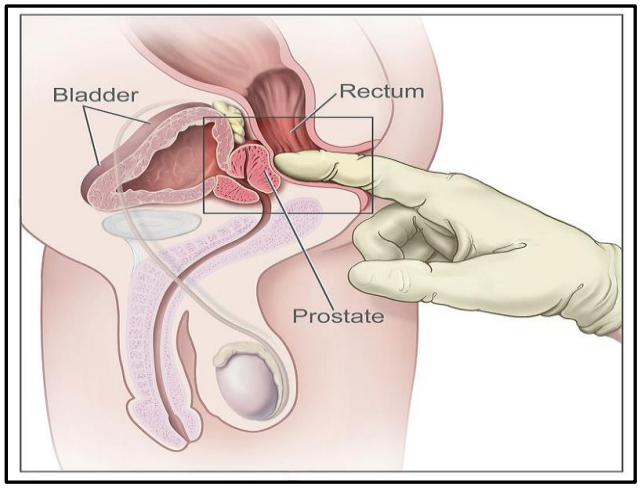

Figure 3: Screening for prostate cancer during a digital rectal examination (DRE) (TeachMe Anatomy, accessed by 01 April 2022).

2.3.3 Prostate Biopsy

A biopsy can be used to confirm the diagnosis in case of any clinical or biochemical suspicions that the patient has prostate cancer. The most typical way to do this is with a tru-cut needle and the transrectal ultrasound-guided method (TRUS) (Weston et al., 2012). To date, transrectal ultrasound guided prostate biopsy is the most frequently utilized (Tops et al., 2022). A prostate biopsy is usually performed under local anesthesia

or sedation. On rare occasions, a general anesthetic is necessary. Traditionally, a sextant biopsy (i.e., six cores) was performed. However, this procedure had a 30 % false negative rate. Hence, an extended biopsy technique utilizing a 12-core biopsy strategy is now advised (Weston et al., 2012).

Currently, a prostate biopsy is indicated for males aged 50 to 69 who exhibit elevated serum PSA levels (> 3 ng/mL) or abnormal digital rectal examination findings (nodules, induration, and asymmetry). For individuals with a previous negative biopsy result, the criteria for repeat biopsy are prolonged rise in blood PSA, worrisome digital rectal examination results, or the presence of atypical small acinar proliferation (Das et al., 2020).

The purpose of a prostate biopsy is to determine the size, grade, and multifocal nature of the tumour, allowing patients and clinicians to forecast a likely course of action more accurately. The downside of this diagnosis method is its side effects. Haematuria; haematospermia; urinary retention; perineal pain; urinary tract infection; and septicemia are among the side effects of prostate biopsy. Table 3, below, highlights these side-effects (Weston et al., 2012).

Table 3: Complications of trans-rectal prostate biopsy (Weston et al., 2012).

Complication	Frequency	Comment
Haematuria	23-63 %	0.7% clot retention
Haematospermia	10-50 %	Up to 6 weeks
Rectal Bleeding	2-21 %	Usually minor
Infection	2.5-10 %	2% needing to be hospitalised
Urinary retention	0.4%	
Vasovagal episode	1.4-5.3%	
Pain		Local anasthetic and/or sedation required

Following a prostate biopsy, fixation of the biopsy is crucial before being sent to the pathologist for histopathological analysis. The following section describes the proper handling and preservation of a biopsy specimen. The study focuses on this process as it is employed in the methodology section.

2.4 Processing of a biopsy specimen:

Following the removal of a biopsy sample, also known as a specimen, it is often preserved by using a neutral-buffered formalin solution, which consists of 3.7-4.0 % formaldehyde buffered with phosphate at a pH of 7 or with 10 % neutral buffered formalin (Buszewska-Forajta et al., 2019). The fixation time should be between 24 to 72 hours, and the formalin should penetrate the entire specimen. The purpose of formalin fixation is to preserve the tissue by inhibiting proteolytic enzymes and microbial growth. The fixed tissue should maintain biological stability during storage (Buszewska-Forajta et al., 2019, Parra-Medina and Ramírez-Clavijo, 2021).

Following formalin fixation, the container is labelled with the patient's name, the area of the biopsy, which is the specific location on the body from which it was obtained, and other details, including the hospital number and the patient's year of birth. When the specimen reaches the lab, the pathologist firstly examines it without using a microscope. This test is commonly referred to as a gross examination. The dimensions, colour, and consistency of the tissue sample, and additional information, is noted during the gross examination. At times photographs may be taken of the specimen, for record keeping (American Cancer Society, accessed 25 September 2023).

Smaller biopsies, such as core needle biopsy or punch biopsy are usually examined under a microscope (American Cancer Society, accessed 25 September 2023). After the gross examination a histological preparation will be prepared. The biopsy tissue is placed in cassettes and placed in a mold with heated paraffin wax following processing (which is often done overnight). The wax solidifies into a block as it cools, shielding the tissue (American Cancer Society, accessed 25 September 2023). The purpose for paraffin embedding is to enhance preservation as well as to make sample sectioning easier (Buszewska-Forajta et al., 2019). Following this, the microtome is then used to slice the paraffin wax block with the imbedded tissue into extremely thin pieces. To alter the tissue's color, a succession of stains or dyes are applied to these thin slices of the material that have been mounted on glass slides. (American Cancer Society, accessed 25 September 2023.

2.5 Histopathology

Histopathology is still the only surefire method of diagnosis, although clinical, biochemical, and radiological factors might lead to a suspicion of prostate cancer. Histopathological analysis can offer crucial prognostic information, in addition to the diagnosis of prostate cancer (Varma and Chandra, 2012). The grade of the prostate cancer is the single most significant pathological prognostic factor. The degree of differentiation visible under a microscope, or how much the tumour resembles the comparable normal tissue, is referred to as tumour grade. Well-differentiated tumours are thought to be low-grade, whereas those that differ significantly are thought to be high-grade or poorly differentiated (Varma and Chandra, 2012).

The Gleason score is the selected grading system which evaluates the likelihood of how quickly the cancer will grow and advance (Cheng et al., 2012). The Gleason system architecture is used to grade prostate tumours (growth mode and level of glandular differentiation) on a prostate cancer pathology scale, using a scale from 1 (the most distinct) to 5 (the least differentiated). A Gleason score is the sum of the primary (most prevalent) and secondary (second-most prevalent) grades if multiple architectural patterns are present in the tumour. For example, the Gleason score is 3 + 4 = 7, when the most prevalent is 3 and the second most prevalent is 4; a Gleason score is 4 + 3 = 7, when the most prevalent is 4 and the second-most prevalent is 3 (Varma and Chandra, 2012).

As a result, rather than using the worst grade, prostate tumours are rated using the average grade. Tumours with a single grade are given a Gleason score for uniformity by doubling the grade (for example, Gleason score 3 + 3 = 6). As a result, Gleason ratings could be between 2 (1+1) and 10 (5+5). Gleason grading is not utilized for other prostate malignancies, such sarcoma, transitional cell sarcoma, or small cell carcinoma; it is solely applicable to prostatic adenocarcinoma. Tumour stage (the extent of the illness both inside and outside the prostate) and tumour volume are additional pathological prognostic variables in prostate cancer (Varma and Chandra, 2012).

2.6 Prostate Cancer Staging

The staging of PCa is important because it highlights the quantity of cancer in the body. It assists in determining the severity of the cancer and the ultimate treatment for its severity. Prostate cancer is categorized into four stages: stage 1 up to 4. It is these stages that enable medical practitioners to estimate the progression of the disease and to make informed decisions about which treatment/s should be administered to the patient (American Cancer Society, accessed 31 May 2021). Currently, the American Joint Committee on Cancer's (AJCC) tumour, node, and metastasis (TNM) staging system is broadly used. The Gleason score and PSA level also form part of the AJCC TNM system (Cheng et al., 2012). Table 4, below, shows the AJCC TNM system.

Table 4: AJCC TNM System (American Cancer Society, accessed 31 May 2021).

AJCC Stage	Tumour Staging	Stage Explanation
I	CT1, NO, MO Grade group 1, PSA<10	cT1 – The oncologist is unable to detect/identify the tumour with a transrectal ultrasound. It is identified through a transurethral resection of the prostate (TURP), or needle biopsy performed for a high PSA.
	OR	
	cT2a, N0, M0 Grade Group 1 PSA < 10	[cT2a] – The tumour can be detected through a DRE or transrectal ultrasound and is situated on one half or less of the prostate. [N0], the cancer has not extended to neighbouring lymph nodes or other body parts [M0]. The grade group equals 1 with a PSA level lower than 10.
	OR	
	pT2, N0, M0 Grade Group 1 PSA < 10	[pT2] – The tumour is extracted surgically, and it is still localized. [N0], the cancer has not extended to neighbouring lymph nodes or other body parts [M0]. The grade group equals 1 with a PSA level lower than 10.
IIA	cT1, N0, MO Grade Group 1 PSA at least 10 but < 20	cT1 – The oncologist is unable to detect/identify the tumour with a transrectal ultrasound. It is identified through a transurethral resection of the prostate (TURP), or needle biopsy performed for a high PSA. [N0], the cancer has not extended to neighbouring lymph nodes or other body parts [M0]. The grade group equals 1 with a PSA level of not less than 10 but lower than 20.
	OR	

	cT2a or pT2, N0, M0 Grade Group 1 PSA at least 10 but < 20	[cT2a] – The tumour can be detected through a DRE or transrectal ultrasound and is situated on one half or less of the prostate. [pT2] - The tumour is extracted surgically, and it is still localized. [N0], the cancer has not extended to neighbouring lymph nodes or other body parts [M0]. The grade group equals 1 with a PSA level of not less than 10, but lower than 20.
	OR	
	cT2b or cT2c, N0, M0 Grade Group 1 PSA < 20	[cT2b] – The tumour can be detected through a DRE or transrectal ultrasound. Its location is more than half of one side of the prostate. [cT2c] – The location of the tumour is on the left and right side of the prostate. [N0], the cancer has not extended to neighbouring lymph nodes or other body parts [M0]. Grade group equals 1 with a PSA level of less than 20.
IIB	T1 or T2, N0, M0 Grade Group 2 PSA < 20	[T1 or T2] – The cancer has not advanced beyond the prostate. It may or may not be detected by DRE or transrectal ultrasound. [N0], the cancer has not extended to neighbouring lymph nodes or other body parts [M0]. Grade group equals 2 with a PSA level of lower than 20.
IIC	T1 or T2, N0, M0 Grade Group 3 or 4 PSA < 20	T1 or T2] – The cancer has not advanced beyond the prostate. It may or may not be detected by DRE or transrectal ultrasound. [N0], the cancer has not extended to neighbouring lymph nodes or other body parts [M0]. Grade group is 3 or 4 with a PSA level of lower than 20.
IIIA	T1 or T2, N0, M0Grade Group 1 to 4 (Gleason score 8 or less)PSA at least 20	T1 or T2] – The cancer has not advanced beyond the prostate. It may or may not be detected by DRE or transrectal ultrasound. [N0], the cancer has not extended to neighbouring lymph nodes or other body parts [M0]. Grade group is 1 to 4 with a PSA level not less than 20.
IIIB	T3 or T4, N0, M0 Grade Group 1 to 4 (Gleason score 8 or less) Any PSA	[T3] – The cancer is no longer confined in the prostate and may have extended to the seminal vesicles. [T4] – The cancer may have extended to neighbouring tissues of the prostate e.g., urethral sphincter, bladder, rectum, and/or the pelvic wall. [N0], the cancer has not extended to neighbouring lymph nodes or other body parts [M0]. The grade group is 1 to 4, whilst the PSA level can be any value.
IIIC	Any T, N0, M0 Grade Group 5 Any PSA	[any T] – The cancer may or may not be advancing beyond the prostate and into neighbouring tissues. [N0], the cancer has not extended to neighbouring lymph nodes or other body parts [M0]. The grade group equals 5 and the PSA level can be any value.

IVA	Any T, N1, M0 Any Grade Group Any PSA	[any T] – The cancer may or may not be advancing beyond the prostate and into neighbouring tissues. [N1], the cancer has advanced to neighbouring lymph nodes, but not other body parts [M0]. The grade group and PSA can be any value.
IVB	Any T, any N, M1 Any Grade Group Any PSA	any T] – The cancer may or may not be advancing beyond the prostate and into neighbouring tissues. [any N], the cancer may or may not have extended to neighbouring lymph nodes, but it has metastasized to other body parts [M1], such as remote lymph nodes, bones or other organs. The grade group and PSA can be any value.

2.7 Prostate Cancer Treatments

There are currently various treatments which are being employed in the fight against localized and metastatic PCa. These include active surveillance, watchful waiting, surgery, radiation therapy, cryotherapy, immunotherapy, hormone therapy, and chemotherapy (Gomella et al., 2009). Even with these advancements in cancer therapy, there are still advantages and limitations with each of these therapies. The study focuses more on hormone therapy and chemotherapy because the patient population in this study were initially treated with hormone therapy as the first line of treatment for localized PCa, and then chemotherapy as the cancer metastasized and progressed to stage IV (known as castration resistant prostate cancer) due to treatment failure. A detailed analysis of these treatments is important, to establish why patients respond differently to the same treatment and the underlying cause of the different treatment outcomes.

2.7.1 Active surveillance

Active surveillance is utilized more in males whose prostate is discovered during the screening test and in older males who do not present any signs or symptoms of the cancer, nor possess other medical conditions. This treatment encompasses closely surveying a patient's condition without administering any treatment until signs or symptoms present themselves (Zerbib et al., 2008).

Between 20 % and 40 % of prostate cancer cases identified by screening may go untreated and asymptomatic until the patient passes away from another reason. However, men with active surveillance, need to have close monitoring so that, in the event

that the tumor progresses, curative treatment can be provided promptly. Individuals with two or fewer positive biopsy cores, GS of six or less, clinically localized prostate cancer, and PSA values less than 10 ng/mL are among those who qualify for active surveillance (Keyes et al., 2013).

2.7.2 Watchful waiting

Watchful waiting (observation) is occasionally used to characterize a less intensive kind of follow-up that can entail fewer testing and a greater reliance on a man's symptom changes to determine whether therapy is necessary. The primary goal of this treatment is usually to manage the cancer's symptoms rather than to treat it (American Cancer Society, accessed 26 November 2023). For elderly people and those with other severe or life-threatening conditions who are projected to live less than five years, this treatment may be an option. Regular PSA testing, DRE, and biopsies are typically avoided with watchful waiting. Treatment to relieve symptoms, such as discomfort or urinary tract obstruction, may be suggested if PCa is the cause of those symptoms. In order to prevent recurring testing and biopsies, patients who begin active surveillance and subsequently have a shortened life expectancy may eventually transition to watchful waiting (Cancer.net, accessed 26 November 2023).

2.7.3 Radical prostatectomy (surgery)

When surgery is used as treatment, only patients who are in good health and whose tumor is localized in the prostate gland are presented with this option to remove the tumor. Surgery, however, is the least preferred option as it presents serious complications which includes impotence, leakage of urine from the bladder or stool from the rectum, shortening of the penis, erectile dysfunction, and inguinal hernia (Zerbib et al., 2008, National Cancer Institute, accessed 17 August 2021).

2.7.4 Radiation therapy

Another treatment option is radiation therapy, which uses powerful radiation to either destroy cancer cells or stop them from proliferating. Men who receive radiation therapy are more likely to develop bladder or gastrointestinal cancer, impotence, and urinary issues that could worsen with age. Radiation therapy is further divided into Brachytherapy and External beam radiation therapy (Zerbib et al., 2008).

2.7.4.1 Brachytherapy

Brachytherapy has become widely accepted and it refers to the positioning of radioactive sources inside or next to a cancer tumour (Keyes et al., 2013). There are two types of brachytherapy: high-dose-rate (HDR) brachytherapy, in which radioactive sources are delivered over the course of approximately ten minutes via temporary catheters, and low-dose-rate (LDR) brachytherapy, in which radioactive seeds are indefinitely embedded into the prostate. In patients with low- or intermediate-risk prostate cancer, low-dose-rate brachytherapy is most frequently used as monotherapy. For patients with high-risk prostate cancer, it is often used in conjunction with External beam radiation therapy (EBRT) (Keyes et al., 2013).

2.7.4.2 External beam radiation therapy

EBRT is a well-established treatment for localized PCa. In intermediate - and high-risk PCa, it is a common treatment strategy when combined with androgen deprivation therapy (ADT) or high-dose-rate brachytherapy. When used in conjunction with brachytherapy, EBRT is thought to be more effective than alone in some high-risk and intermediate-risk patients (Keyes et al., 2013).

2.7.5 Cryotherapy

Cryotherapy is a treatment that launches a probe into the prostate tumour and freezes it, thereby destroying the cancer cells. The complications accompanying cryotherapy

include impotence, incontinence, and tissue sloughing (Shelley et al., 2007). This treatment option is still being studied in clinical trials.

2.7.6 Immunotherapy

Another treatment option is Immunotherapy. Immunotherapy utilizes specific drugs to prompt an individual's own immune system to recognize and kill cancer cells more successfully. Side effects can include fatigue, nausea, itching, skin rash, decrease of appetite, constipation, joint pain, and diarrhea (American Cancer Society, accessed 17 August 2021).

2.7.7 Hormone therapy

Hormone therapy is also referred to as androgen deprivation therapy (ADT). The objective of ADT is to decrease the levels of testosterone and dihydrotestosterone, which are also called androgens, in the body, or to prohibit them from stimulating the growth of PCa cells (American Cancer Society, accessed 23 July 2021). The testicles are mainly responsible for the production of androgens. However, the PCa cells and the adrenal glands can also produce a fair amount. Cessation of endogenous androgen secretion or a decrease thereof often contributes to PCa diminishing or growing slowly (American Cancer Society, accessed 23 July 2021).

One of the drugs that stops the generation of androgens by these cells is Abiraterone (American Cancer Society, accessed by 23 July 2021). Abiraterone is an oral inhibitor in the biosynthesis of testosterone and dihydrotestosterone and exerts its effect through inhibiting cytochrome P450 17 (17α – hydroxylase – 17, 20 – lyase), the principal enzyme in the biosynthesis of androgens (Abidi, 2013). The following side effects may accompany this hormone therapy in men, namely: hot flushes; impotence; osteoporosis; gynecomastia; diarrhoea; nausea, and itching (Savard et al., 2013).

Hormone therapy is utilized as a curative therapy for males with high-risk localized, and recurring PCa, and for palliative care in men with metastatic PCa (Narayan et al., 2021).

Additionally, chemotherapy continues to be the mainstay therapy for castration resistant PCa (CRPC) (Mahon et al., 2011).

2.7.8 Chemotherapy

Chemotherapy is the treatment option that utilizes drugs to block the growth of cancer cells by killing the cells or preventing them from dividing. Chemotherapy is the most used treatment option, despite its unbearable side effects. Some of the side effects following chemotherapy include hair loss, nausea and vomiting, fatigue, and infections (American Cancer Society, accessed by 23 July 2021).

Chemotherapy involves anti-cancer drugs being administered to the patient, orally or intravenously. This therapeutic treatment is often employed when aggressive PCa cells progress beyond the prostate to other body parts. Chemotherapeutic treatment can be administered as a single drug, or a combination of chemo drugs (combination therapy). Some of the drugs commonly used in the treatment of PCa are docetaxel, cabazitaxel, mitoxantrone and estramustine (Gilligan and Kantoff, 2002, Calabrò and Sternberg, 2007). Generally, the initial chemo drug administered is docetaxel, in isolation, or in combination with the steroid drug prednisone (American Cancer Society, accessed by 23 July 2021). This study provides more literature on docetaxel as the main drug for the treatment of PCa in Bloemfontein, Free State Province, South Africa.

2.8 Chemotherapeutic agents used in PCa

2.8.1 Docetaxel

Docetaxel is a second-generation taxane, extracted from a compound in the European yew tree (*Taxus baccata*). This drug exhibits powerful and wide chemotherapeutic properties (Varnai et al., 2019). According to studies in which docetaxel was utilized in isolation, it displayed an equitable response rate in 38 % of patients, accompanied by a PSA decrease of above 50 % in 69 % of patients (Nader et al., 2018). Docetaxel was given clearance by the Food and Drug Administration (FDA) for its use in conjunction with

prednisone for treating metastatic androgen-independent prostate cancer (AIPC)/ hormone-refractory prostate cancer (HRPC) (Teply et al., 2016).

Docetaxel's method of action includes binding to, and stabilizing, β-tubulin, which inhibits microtubule disintegration and causes cell cycle arrest at the G2/M phase, as well as apoptosis. Cytochrome P450 enzymes; CYP3A4 and CYP3A5 are responsible for metabolizing docetaxel (Varnai et al., 2019). Moreover, docetaxel is the substrate for ABCB1, ABCG2, ABCC1 and ABCC2 multi-drug transporters (Varnai et al., 2019).

2.8.1.1 Effect of docetaxel on castration-sensitive and castration-resistant metastatic PCa

Castration-sensitive metastatic prostate cancer (mCSPC) and castration-resistant metastatic prostate cancer (mCRPC) are the two types of metastatic prostate cancer; most mCSPC cases eventually advance to mCRPC after becoming resistant to first-line hormonal treatment (Quinn et al., 2017). High androgen levels are required by prostate cancer cells in mCSPC to fuel the malignancy's growth. Consequently, the first course of ADT treatment will be effective for about 90 % of patients with mCSPC. ADT for mCSPC functions by reducing androgen production in the testes (Hahn et al., 2018). The introduction of medicines, such as docetaxel or abiraterone, to ADT for a more severe upfront treatment of metastatic prostate cancer results in further significant improvement in the outcome of patients with mCSPC (Hahn et al., 2018).

While many chemotherapeutic medications have been studied in mCRPC, docetaxel was the first to demonstrate a statistically significant improvement in overall survival. Docetaxel is still widely utilized as the recommended first-line treatment for mCRPC, despite the fact that the survival improvement seen in this condition was brief (two to three months), yet noteworthy (Lima et al., 2021). Nevertheless, despite the improved efficacy of docetaxel-based treatment, about half of the patients do not improve, and those who do, eventually become resistant to the drug. To counter for this, cabazitaxel, a second-generation taxane has been shown to produce clinical responses, enhance overall survival, and combat docetaxel resistance (Quinn et al., 2017).

2.8.2 Cabazitaxel

Cabazitaxel, which is also a second-generation taxane, was approved for use in PCa by the FDA in 2010. It is utilized in combination with prednisone for the treatment of hormone-refractory metastatic PCa in patients whose illness has advanced following previous treatment with docetaxel-based therapy (Abidi, 2013). Cabazitaxel acts on docetaxel-sensitive and docetaxel-resistant tumours due to its lower affinity for P-glycoprotein (P-gp), compared to paclitaxel and docetaxel (Sun et al., 2018). Cabazitaxel was developed following resistance to docetaxel and paclitaxel. It was observed to be as potent as docetaxel in cell lines, and displays antitumour activity in models that presented resistance to other taxanes (Nader et al., 2018).

2.9 Chemoresistance in cancer

Among a variety of available cancer treatments, chemotherapy is well known for its efficacy. Chemotherapy, however, is challenged by tumours which develop resistance to chemo drugs. Tumour resistance can either be intrinsic, due to genetic traits of the tumour, or acquired in the presence of the chemo drug. Chemoresistance leads to treatment failure; disease relapse; cancer progression; consequent deterioration of the patient's health; and ultimately mortality (Zheng et al., 2020). There are several molecular aspects which contribute to multi-drug resistance. In the case of cancer, these include "transporter pumps; oncogenes (EGFR, PI3K/Alt, Erk and NF-κB); tumour suppressor genes (p53); mitochondrial alteration; DNA repair; autophagy; epithelial mesenchymal transition (EMT); cancer stemness, and exosome" (Zheng et al., 2020). Of all these molecular mechanisms which contribute to multi-drug resistance, transporter pumps are the most common mechanism of drug resistance that has been extensively studied. The main contribution of transporter cellular pumps in chemoresistance is in reduction of intracellular concentrations of anticancer drugs (Kachalaki et al., 2016).

Although the precise mechanisms by which PCa develops resistance to docetaxel remains unclear, several mechanisms of resistance were established in earlier research (Lima et al., 2021). These pathways include adjustments to cell death mechanisms like

autophagy and apoptosis; ß-tubulin; altered AR signaling; and increased intracellular drug activity by ABC transporter members (Lima et al., 2021). A closer look at the structures, function and mechanisms of these transporter pumps and their correlation to chemoresistance is explored in the following section.

2.10 Transporter pumps and chemoresistance

The ABC transporter family of transmembrane proteins is composed of 49 transporters which are further divided into seven categories, ABC-A to -G, based on sequence similitude. ABC transporters account for the transport of several substrates, such as xenobiotics; amino acids; sugars; ions; lipids, and peptides, over the plasma membranes through the ATPase transporter or channel proteins (Zheng et al., 2020). The ABC transporters' structure is composed of at least two nucleotide-binding domains (NBD) and two transmembrane domains (TMD). The TMDs are responsible for translocating several substrates over the plasma membrane by way of conformational changes, whilst the NBDs have an ATP-binding site (Zheng et al., 2020).

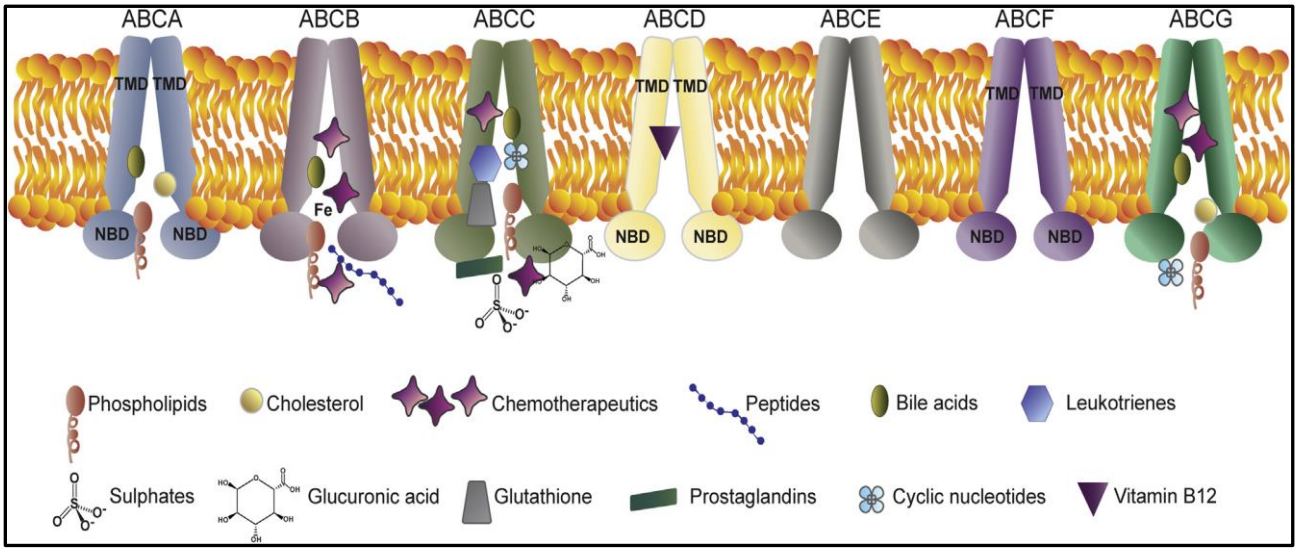

Figure 4: ATP-binding cassette family divided into seven classes ABC-A to -G (Domenichini et al., 2019).

A significant role in drug metabolism is played by ABC transporters. These transmembrane proteins can impact the effectiveness of chemotherapy because they are involved in the transport of physiologically significant substrates, such as anti-cancer drugs across cell membranes (Sone et al., 2019) . Three members of the ABC superfamily, namely P-glycoprotein (ABCB1), MRP1 (ABCC1) and ABCG2, are multidrug efflux pumps whose expression is accountable for chemoresistance (Sharom, 2008). The increased expression of ABC transporters, for example, might increase drug efflux while decreasing cytoplasmic drug concentration, resulting in decreased efficacy and possibly a drug resistant phenotype (Sone et al., 2019). The efflux transporter ABCC2 has been shown to play a significant role in the metabolism of docetaxel. In addition, it has been documented that ABCC10/multidrug resistance protein 7 (MRP7), can give resistance to anti-tubulin drugs such as taxanes (Sone et al., 2019). The multidrug efflux pumps, ABCC1, ABCC2 and ABCC10 genes, are the transporters of interest in this study, as a mechanism of resistance to PCa treatment.

2.10.1 Multidrug resistance associated proteins (MRPs)

The MRP (multi-resistance associated protein) subfamily is made up of 13 members, nine of which are essentially involved in multidrug resistance (MDR). These nine MRPs are accepted as ATP-dependent efflux transporters for foreign and endogenic substances, based on their location and functional characterization, and on cloning studies (Sodani et al., 2012). ABCC1, ABCC2, and ABCC10 will be closely investigated because these transporters efflux various chemo drugs, including docetaxel, which is the drug utilized in PCa treatment, and chosen for this study.

2.10.1.1 ABCC1 gene (associated protein is MRP1)

The ABCC1 gene was the initial ABC-transporter gene cloned in the ABCC1 proteins and was seen to be greatly overexpressed in the cell line of the human lung carcinoma H69AR, which is doxorubicin-resistant (Chen and Tiwari, 2011, Chen et al., 2021). This protein has a molecular weight of 190 kDa and its structure differs from P-glycoprotein because it contains an additional MSD, termed MSD_0, with five transmembrane (TM)

helices, and two additional MSDs, each containing six TM helices with two nucleotide binding domains (NBD) in the middle. The purpose of the NBDs is to act as a source of energy to create hydrolyzed ATP, whilst the MSDs support dimerization, drug binding, trafficking, and putative drug transport channels (Sodani et al., 2012, Domenichini et al., 2019, Chen et al., 2021).

This ABC transporter is mainly expressed in the spleen; colon; breasts; kidneys; testes; lymph nodes; blood brain barrier; pancreas; brain; and liver. Furthermore, in normal physiological conditions it exports the following natural substrates: leukotriene C4 (LTC4); glutathione; lysophosphatidylinositol (LPI); glutathione disulphide; prostaglandins; sphingosine-1-phosphate; and $E_2$17βG (estradiol glucuronide). Increased MRP1 levels have been observed in several cancer types, which include PCa; non-small cell lung cancer (NSCLC); breast cancer; ovarian cancer; leukaemias; melanomas; gastrointestinal carcinomas; and esophageal carcinomas (Chen and Tiwari, 2011, Sodani et al., 2012, Domenichini et al., 2019, Chen et al., 2021). MRP1 bestows multidrug resistance on anthracyclines; vinca alkaloids; camptothecins; daunorubicin; imatinib; etoposide; vincristine; vinblastine; and methotrexate in tumour cells (Domenichini et al., 2019, Sodani et al., 2012, Chen and Tiwari, 2011).

Expression of MRP1 has been associated with clinical outcomes. However, the general input of MRP1/ABCC1 to clinical drug resistance is still not clear, even though MRP1 protein and/or mRNA have been regularly detected in the tumour samples of patients (Chen and Tiwari, 2011).

2.10.1.2 ABCC2 gene (associated protein is MRP2)

The second member of the nine MRPs involved in MDR is MRP2 with a molecular weight of 174 kDa. It was initially reproduced from rat hepatocyte and was termed hepatocellular canalicular multiple organic anion transporter (cMOAT). Its amino acid is 49 % the same as that of MRP1, but contains a dissimilar expression pattern (Chen and Tiwari, 2011, Sodani et al., 2012). Due to MRP2 being responsible for an array of conjugates, like to those of MRP1, it is also believed to confer resistance to similar chemotherapeutic drugs (Sodani et al., 2012).

MRP2 is mainly expressed in the pancreas; lymph nodes; liver; brain; liver; testes; colon; lungs; and breasts. In normal physiological conditions, it transports sulfate conjugates; leukotriene C4 (LTC4); glucuronate; bilirubin; glutathione; and $E_2$17βG. MRP2 has been expressed in colorectal, liver, lung, and gastric cancer cell lines, as well as in Dubin-Johnson syndrome. It transports and confers resistance to vincristine; doxorubicin; topotecan; carboplatin; irinotecan; cisplatin; paclitaxel; vinblastine; and epirubicin (Chen and Tiwari, 2011, Sodani et al., 2012, Domenichini et al., 2019).

2.10.1.3 ABCC10 gene (associated protein is MRP7)

The 160 kDa, MRP7, consists of three MSDs and two NBDs (Hopper-Borge et al., 2009, Sone et al., 2019). In comparison with other members of the MRP family, MRP7 was shown to have the lowest amino acid sequence identity (33-36 %). However, MRP7 protein displays a membrane structure resembling MRP1 and MRP2 in that it has three MSDs organized around its 17 TM helices (Chen and Tiwari, 2011).

MRP7 is a lipophilic anion transporter which also confers resistance to numerous natural product chemotherapeutic drugs. MRP7's role in conferring resistance to vincristine; docetaxel; vinblastine; and paclitaxel has been documented in an *in vitro* study (Chen and Tiwari, 2011). Thus far, a clinical study to establish the role of MRP7 in clinical drug resistance has not been documented (Chen and Tiwari, 2011).

CHAPTER 3:

RESEARCH METHODOLOGY

3.1 Ethics Clearance

The ethics approval for this study was obtained from the Health Sciences Research Ethics Committee at the University of the Free State (ethics approval reference number UFS-HSD2022/1325/3101). The approval to conduct studies using PCa patients' needle biopsies and data from the specified hospitals was obtained from the Free State Department of Health and the National Hospital's head of oncology. Approval was also obtained from the AARMS (Academic Affairs and Research Management System) (reference number PR2343021), which is a division of the NHLS responsible for research management and access to archived biological materials.

3.2 Study Design

The study is an *in vitro* retrospective study which investigated ten archived tissue samples of biopsies obtained from ten PCa patients. The ten samples were divided into two categories: five as good responders, and five as poor responders, based on the clinical data of patients. Patients in the good responder category are those who displayed symptomatic improvement after treatment, and whose disease did not progress for more than six months. The poor respondent's category includes patients who did not present any symptomatic improvement, and whose disease advanced. The results obtained from the downstream experiments were analyzed comparatively. Figure 5, below, summarises the study design.

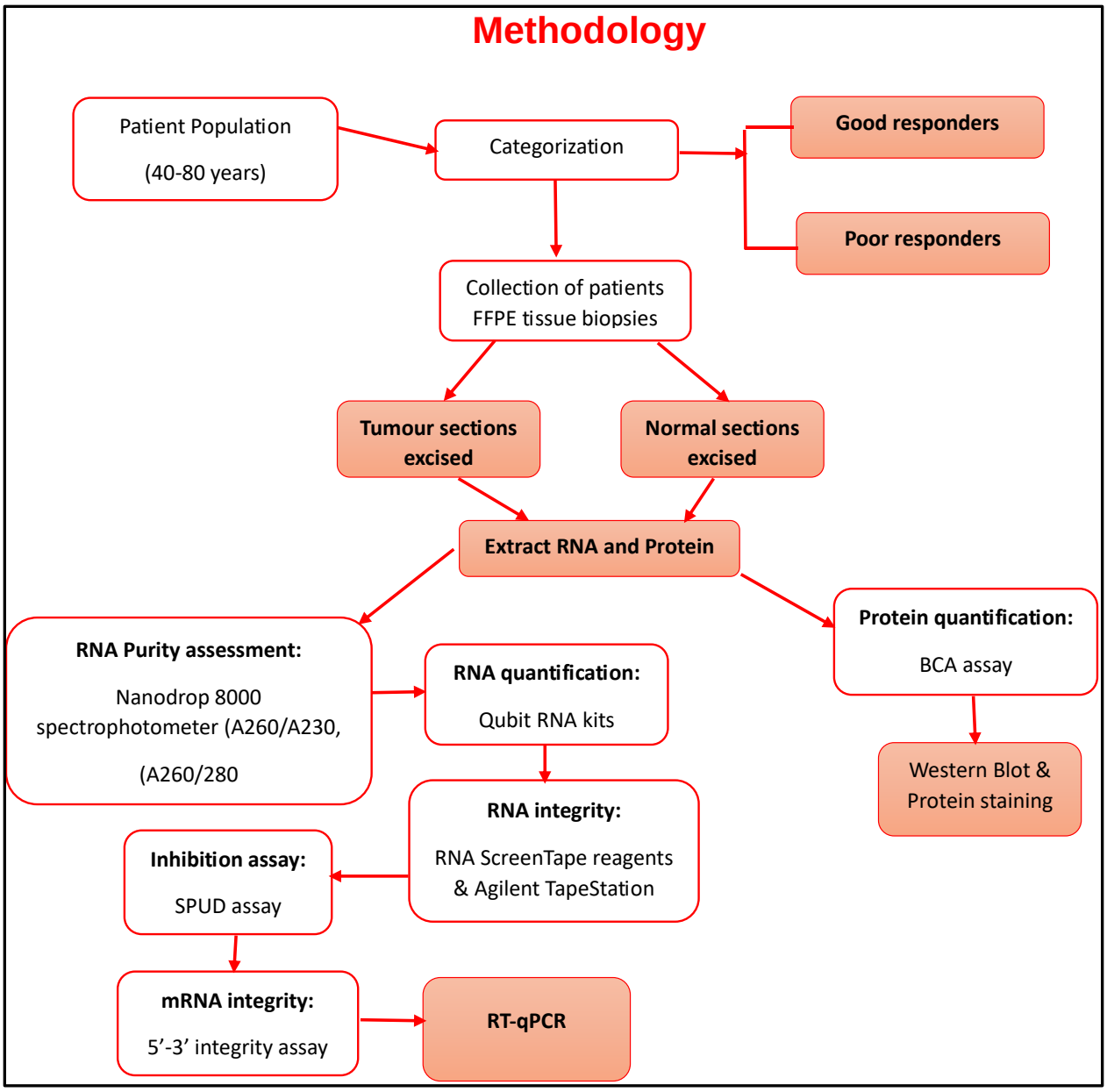

Figure 5: Overview of the study design.

3.3 Research Team Involved in the Study

The research team consisted of the principal investigator, an Anatomical Pathologist, a Biomedical Scientist, and a Pharmacologist. The principal investigator was responsible for obtaining anonymized archived FFPE PCa tissue samples from a similar previous study; extracting RNA and proteins from the samples; carrying out quantification and expression experiments; and analyzing the results using GraphPad prism software. The anatomical pathologist examined the tissue samples under the microscope, and identified and marked the malignant and normal cells areas from the tissue biopsies of different patient categories, based on histopathological data (tumour, node, metastasis) (TNM) staging system. The expertise of a Biomedical Scientist and Pharmacologist guided the RNA and protein extractions, results analysis, and correlating gene expression data with PCa patients' treatment responses.

3.4 Patient Population, Data Collection and Categorization

An oncologist, who was not part of the project, utilized patient clinical records to identify patients who fell into the two categories. Thereafter she provided anonymized, coded sample numbers for the FFPE biopsies of the patients in the good and poor responder categories. These samples were archived at the NHLS located at the Universitas Academic Hospital in Bloemfontein, Free State. The principal investigator in this research study received the above-mentioned samples from a linked study. The oncologist held the patients' identity code.

Histopathological analysis was conducted by determining the percentage of tumour, the areas of malignant and normal cells, and the Gleason score, in each tissue biopsy. See Figure 6, below, which displays FFPE histology slides with areas of interest marked.

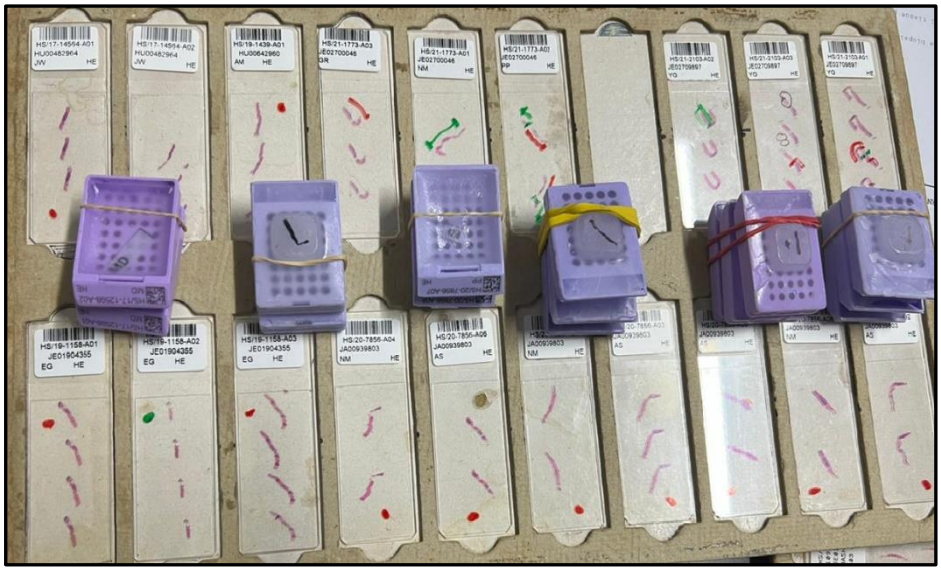

Figure 6: Histology slides: These slides were viewed under a microscope to identify areas of interest. The red marker indicates area/s of malignant cells, and the green marker indicates area/s of normal cells. Each histology slide has a tissue biopsy wax block (purple cassettes) from which the area of interest was excised.

The FFPE tissue biopsies were obtained from prostate cancer patients, between the ages of 40 and 80 years. The samples were sourced from retrospective data collected during the period of 01 January 2015 – January 2022, from patients who had received two-to-ten cycles of docetaxel treatment and archived at NHLS. The patients who presented a positive treatment outcome (sensitive to treatment) were categorized as good responders. Those who displayed a negative prognosis (resistant to treatment) fell in the poor responder category. A sensitive-to-treatment outcome signifies that there was an improvement in the symptoms of the patient for more than six months; a decrease in the PSA level of the patient; no detectable cancer; or the treatment caused the tumour to shrink and its spread halted. Resistance to treatment outcome indicates that the treatment did not improve the symptoms of the patient; the PSA level of the patient did not decrease; or the disease had advanced.

Ten FFPE biopsy blocks were collected for ten different patients, five per group, according to the above-mentioned category specifications. However, after consultation with the Anatomical Pathologist, one of the patients in the good responder category was excluded.

This changed the experimental group design and reduced the total number of patients in these two categories, to nine. The reason for the exclusion of this patient sample, was because histopathological analysis showed 100 % tumour on the FFPE tissue biopsy of this patient. Therefore, no normal tissue could be excised from the tissue sample. Due to this, no comparison would be drawn between the tumour and normal sections of this patient in downstream applications. As a result of this limitation, the patient was excluded.

From each FFPE tissue block, two sections, a normal section (free of PCa) and a tumour section were excised. In total, 18 sections were excised from the nine FFPE tissue blocks of the different patients. The normal, healthy tissue was used as the control. The tissue specimens were sectioned at 6 µm – 10 µm using a microtome. After excising the areas of interest, they were placed in nuclease free tubes and labeled with green and red stickers, as well as numbers which correspond with the patient's sample number. See Figure 7 below.

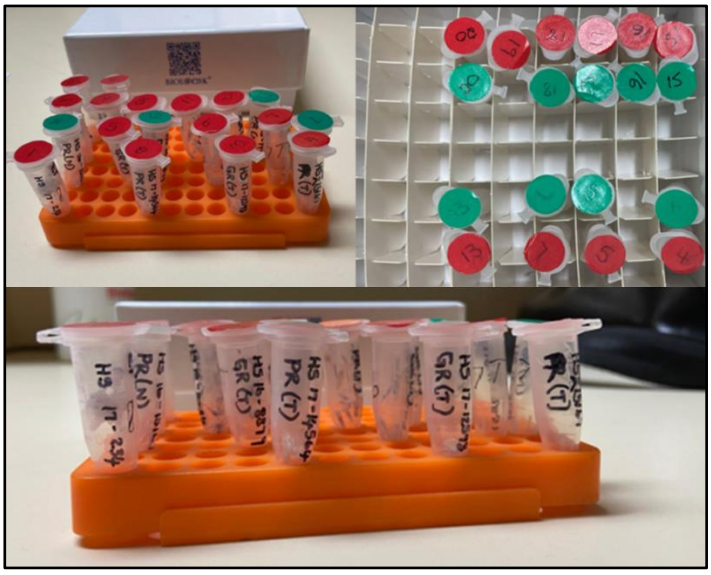

Figure 7: Nuclease-free tubes containing FFPE tissue samples of patients. Each tube contains thinly excised rolled-up tissue. Red stickers mark a tumour section, and green stickers, normal cells, which serve as the control.

The formalin-fixed, paraffin-embedded prostate tissue in nuclease free tubes was stored at room temperature until analysis. Table 5, below, provides the clinical characteristics of

the ten patients, which corresponds to the ten FFPE tissue blocks, with treatment outcomes which fall into the two specified categories.

Table 5: Clinical characteristics of prostate cancer patients (good and poor responders). Clinical data obtained from the oncology center at National Hospital in Bloemfontein, Free State.

Patient Categories					
Good Responders	**HS/21-2103**	**HS/19-1158**	**HS/18-7520**	**HS/16-8879**	
Clinical stage	IV	IV	IV	IV	
Symptomatic improvement	Yes	Yes	Yes	Yes	
Gleason Score (GS)	8 (4+4)	7(4+3)	7(4+3)	7(3+4)	
Grade group (Gg)	4	3	3	2	
Serum PSA Level	8320 ng/ml	4514	7µg/l	n/a	
Number of cycles of Docetaxel (months)	2-10	2-10	2-10	2-10	
Progressive disease	No	No	No	No	
Age	55	53	57	66	
Excised tissue: Tumour (T)/Normal (N)	T & N	T & N	T & N	T & N	
Poor Responders	**HS/21-1773**	**HS/19-11900**	**HS/18-13038**	**HS/16-2331**	**HS/16-15167**
Clinical stage	IV	IV	IV	IV	IV
Symptomatic improvement	No	No	No	No	No
Gleason Score (GS)	8(4+4)	8(5+3)	8(4+4)	9(4+5)	7(4+3)
Grade group (Gg)	n/a	4	4	4	3
Serum PSA Level	n/a	9287	2874 µg/ml	1080	75 ng/ml
Number of cycles of Docetaxel (months)	2-10	2-10	2-10	2-10	2-10
Progressive disease	Yes	Yes	Yes	Yes	Yes
Age	68	67	57	61	56
Excised tissue: Tumour (T)/Normal (N)	T&N	T&N	T&N	T&N	T&N

3.5 FFPE Tissue Processing – Total RNA and Protein Extraction

This section covers the extraction of the total RNA, and proteins from FFPE tissue biopsies, which were later used for proteomic and genetic analysis of the expression of ABC-transporter genes. The protocol utilized was employed from Zymo research's Quick-DNA/RNA™ FFPE kit with catalog number #R1009.

3.5.1 Materials

Nuclease free tubes were utilized to contain the microtome sections which were excised from the patients' FFPE tissues. Digital heatblock (Benchmark, USA) was used during tissue digestion of the samples. A Gilson vortex machine (GV Lab, Germany) was used

for proper mixing of the solutions. A centrifuge machine (Hermle Z32 HK, Germany) was used to separate the components in the tissue solutions, as well as remove insoluble debris. The Zymo Spin IICR columns and collection tubes (Zymoresearch, USA) were used to spin down and extract the RNA from the tissue biopsies. A -80 ^{0}C freezer was used to store the extracted RNA until analysis. These are standard materials which were also used in the protein extraction method.

The following solvents were used during the extraction procedure: the deparaffinization solution, to remove the paraffin wax embedded in the tissue samples. The 2x digestion buffer and proteinase K were used for tissue digestion. The DNase/RNase free water was utilized to prevent RNA sample loss. DNA/RNA lysis buffer was used during DNA/RNA purification to lyse the tissues, deactivate the RNases, and preserve the RNA. The washing buffer was used to ensure that all impurities, such as proteins which also tend to attach non-specifically to the silica membrane, were eliminated. In addition, the prep buffer was used for purification of the RNA. The DNase I and the DNA digestion buffer were used during the DNase I treatment to remove contaminating DNA, along with the DNase used to destroy it. All these solvents were part of the Quick DNA/RNA FFPE kit (Zymoresearch, USA).

3.5.2 Total RNA extraction from FFPE tissues of patient samples

Aliquots of 400 µl of the deparaffinization solution were added to the nuclease-free tubes containing the samples and incubated at 55 ^{0}C for 1 minute. Thereafter, the samples were vortexed. The following mixture was added to the deparaffinized tissue samples per sample: DNase/RNase-Free Water (95 µl), 2x digestion buffer (95 µl), and proteinase K (10 µl). This mixture was made in a nuclease-free tube prior to being added to the samples. Thereafter, the samples were incubated at 55 ^{o}C for 1 hour. This was followed by another incubation at 94 ^{0}C for 20 minutes to de-crosslink the samples. After incubation, 600 µl of the DNA/RNA lysis buffer was added to each tissue sample and mixed thoroughly. The samples were then centrifuged at 16,000 x g for 1 minute to remove the insoluble debris. After centrifugation, the supernatants were transferred to

Zymo-Spin IICR columns in a collection tube and centrifuged for 30 s at 16,000 x g. The flow-through obtained from centrifugation was saved to be used in the RNA purification.

The flow-through obtained in each sample was transferred to new nuclease-free tubes. Ethanol (100 %) was added to the flow-through (1:1) and mixed well. After thorough mixing, the samples in each tube were transferred into new Zymo-Spin IICR columns in a collection tube and centrifuged for 30 s for RNA-binding. The flow-through was removed from the columns and transferred into new nuclease tubes for storage at -80 ^{0}C. It was used for proteomic analysis (protein quantification and western blotting) as it contained proteins.

Following the above RNA-binding step, 400 µl of DNA/RNA wash buffer was added to the column, centrifuged for 30 s, and the flow-through discarded. For each sample to be treated, DNase I reaction mix was prepared in a new nuclease-free tube. The mixture was composed of DNase I (5 µl) and DNase digestion buffer (75 µl) per sample and mixed by gentle inversion. Thereafter the mixture was added into each column matrix and incubated at room temperature (20 ^{0}C – 30 ^{0}C) for 15 minutes.

After incubation, 400 µl of DNA/RNA prep buffer was added to each sample column and centrifuged for 30 s. The flow-through was discarded. Thereafter, 700 µl DNA/RNA wash buffer was added to each sample column and centrifuged for 30 s. The flow-through was discarded. Following this, 400 µl DNA/RNA wash buffer was added to each sample column and centrifuged for 1 minute to ensure complete removal of the wash buffer. The columns were each transferred into new nuclease-free tubes. Thereafter, 50 µl DNase/RNase-free water was added directly to the column matrix and centrifuged for 30 s. The flow-through containing the RNA was stored at -80 ^{0}C until analysis.

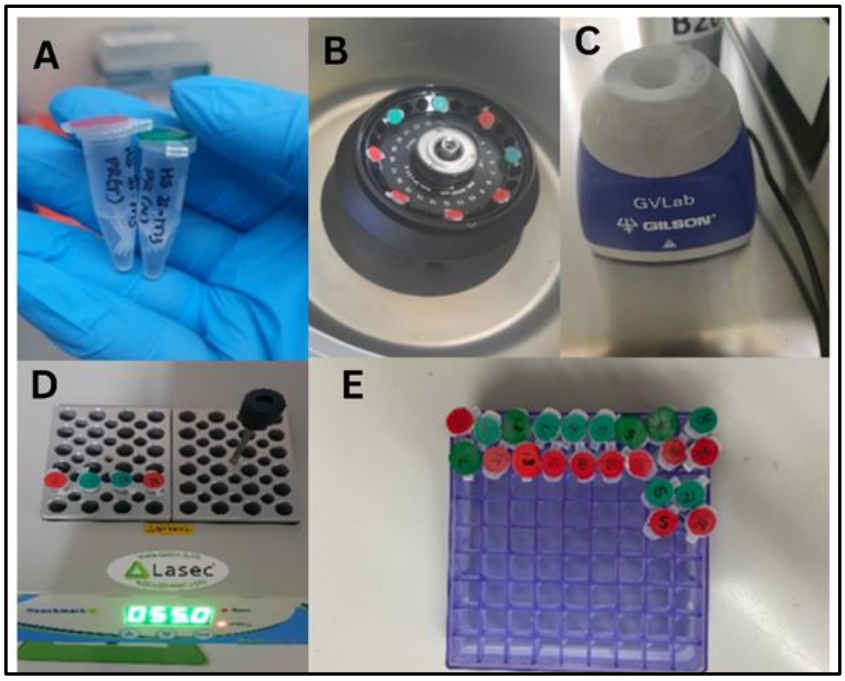

Figure 8: Steps involved in RNA extraction: A - deparaffinization; B - centrifugation; C - vortexing; D - incubation; E - storage of extracted RNA in -80 ^{0}C freezer.

3.6 RNA Quantification and Purity Assessment

FFPE RNA quantity and A260/A280 and A260/A230 purity ratios were obtained using a NanoDrop 8000 spectrophotometer (Thermo Fisher Scientific). RNA concentrations were also quantified by Qubit RNA High Sensitivity Kit and a Qubit 4 instrument.

3.7 RNA Integrity TapeStation Analysis

FFPE RNA integrity was assessed using a 4200 TapeStation RNA ScreenTape and RNA high sensitivity ScreenTape (Agilent Technologies) capillary electrophoresis systems, according to the manufacturer's instructions. The RIN and DV200 were measured using the TapeStation analysis software 5.1.

3.8 SPUD qPCR Inhibition Assay

The SPUD assay was performed, as reported by (Nolan et al., 2006). Briefly, a 100 µM stock solution of the 101 bp SPUD template (Integrated DNA Technologies) was serially diluted ten-fold to a working concentration of 10− 5 nM (10th dilution in the series). Two µl of the diluted template, 0.25 µM of both forward and reverse SPUD primers (IDT), and 1x PowerUp SYBR green master mix (Thermo Fisher) were combined with 1 µl of the FFPE RNA in a total volume of 10 µl in a MicroAmp Optical 384-well reaction plate (Thermo Fisher). Negative inhibition control was prepared by replacing the RNA samples with nuclease-free water. All samples were analysed in triplicate. The plate was sealed with the MicroAmp optical adhesive film (Thermo Fisher), and qPCR reactions were conducted using the QuantStudio 12K flex real-time PCR system (Thermo Fisher) with the following cycling conditions: 95 °C for 10 min; followed by 40 cycles of denaturation at 95 °C for 15 s; and annealing/elongation at 60 °C for 1 min. Fluorescence data was recorded every cycle at the end of the annealing/elongation step at 60 °C. This cycling was followed by a melt curve analysis of 95 °C, then a gradient going from 60 °C to 95 °C in 0.05 °C increments. Data was analysed using the QuantStudio 12K flex software v1.2.4 and Cq values were exported to Microsoft Excel for further calculations to compare Cq values of all the samples to identify potential reaction inhibition.

3.9 5’-3’ Integrity Assay

Oligo(dT)-primed cDNA was prepared using the Superscript IV first-strand synthesis kit (Thermo Fisher Scientific) and 100 ng total RNA, according to the manufacturer’s specifications. Real-time qPCR amplifications were performed in 10 µl containing 5 µl 2x PowerUp SYBR green master mix (Thermo Fisher), 0.5 µl forward and reverse primer (500 nM final concentration), 2 µl nuclease-free water and 2 µl cDNA. The cycling conditions comprised of 2 min UDG activation at 50 °C; 2 min polymerase activation at 95 °C; 40 cycles of 15 s at 95 °C, and 1 min at 57 °C, followed by a dissociation curve analysis. The two primer pairs used for qPCR targeted the 3’ end (3’ GAPDH qPCR assay) and 5’ start (5’ GAPDH qPCR assay) of the reference gene GAPDH (Nolan et al.,

2006). The GAPDH 3' and 5' Cq values were determined for each sample and the difference in Cq value (ΔCq5'-3') was calculated for each sample.

3.10 Primer Design for qPCR

Primer design for qPCR primers for the target genes, ABCC1 and ABCC2 were designed using the NCBI primer blast software (http://www.ncbi.nlm.nih.gov/tools/primer-blast/), using the parameters shown in Table 11 to give 80 – 200 bp amplicons. The primers for GAPDH, HPRT1, and HSPCB were sourced from the literature and had been validated. The primer sequences for ABCC10 were obtained from the PrimerBank database (https://pga.mgh.harvard.edu/primerbank/).

3.11 Primer Preparation

The qPCR primers were sourced from IDT and were resuspended in TE buffer (10 mM Tris, pH 8.0, 1 mM EDTA) to a 100 µM stock concentration, as per manufacturer instructions.

3.12 cDNA Synthesis

cDNA was synthesized from 100 ng FFPE total RNA using the Maxima H Minus cDNA synthesis master mix with dsDNase kit, according to the manufacturer's protocol (Thermo Fisher Scientific Pub. No. MAN0016393, Rev.B.0). A 1 µg of a commercial XpressRef universal total RNA (QIAGEN) was also reverse transcribed and used for validation of the qPCR assays and as a positive control. NRT negative control reactions were performed alongside to assess for genomic DNA contamination of the RNA sample. An NTC reaction was also included to assess for reagent contamination and primer dimers.

3.13 cDNA Preamplification

For FFPE cDNA pre-amplification, the TaqMan PreAmp master mix (Thermo Fisher) was used according to the manufacturer's instructions. All qPCR primers were pooled by combining 1 µl of each 100 µM primer stock to make a final volume of 200 µl in TE buffer to give a final concentration of 500 nM of each primer. The preamplification reaction was performed in a final volume of 5 µl containing 2.5 µl TaqMan PreAmp master mix, 0.5 µl pooled primer mix and 2 µl cDNA, and amplified using the cycling conditions: one cycle at 95 °C for 10 min; 14 cycles at 95 °C for 15 s; and 60 °C for 4 min. At the end of the cycling programme, the reactions were diluted 1:20 in TE buffer. Pre-amplified DNAs were stored at −20 °C until used for qPCR assays.

3.14 qPCR Validation

3.14.1 qPCR reaction efficiency

PCR efficiency was determined using standard curves generated with two- and ten-fold dilutions of the XpressRef universal total cDNA for each target gene. Real-time qPCR amplifications were performed in triplicate in 10 µl volume containing 5 µl 2x PowerUp SYBR green master mix (Thermo Fisher); 0.5 µl forward and reverse primer (in a 500 nM final concentration); 2 µl nuclease-free water; and 2 µl cDNA. The reactions were performed on the QuantStudio 12K flex PCR system (applied biosystems) using the following cycling conditions: 2 min UDG activation at 50 °C; 2 min polymerase activation at 95 °C; 40 cycles of 15 s at 95 °C; and 1 min at 57 °C, followed by a dissociation curve analysis. Standard curves were generated by plotting the CT values against the log of each serial dilution.

3.15 qPCR Assays

qPCR was performed in a total reaction volume of 10 ul, consisting of 2 µl diluted preamplified cDNA as a template; 5 µl of 2x PowerUp SYBR green I master mix (Thermo Fisher); and both the forward and reverse primers, to a final concentration of 500 nM. NTC reactions were included in all assays as negative controls. Each reaction was run in triplicate. Reactions were performed on the QuantStudio 12K

flex real-time PCR System (applied biosystems), using the following cycling parameters: 50 °C for 2 min; initial denaturation at 95 °C for 2 min; followed by 40 cycles of 95 °C for 15 secs, and 57 °C for 1 min. A melt curve analysis was performed on all reactions at the end of the PCR run using default parameters. Amplification data were analyzed with Life Technologies QuantStudio 12K flex software v1.2.4, applying user-defined thresholds to obtain Cq-values. Outliers in technical replicate reactions, reactions that showed no amplification, and reactions that showed multiple Tm peaks during melt curve analysis were removed from the analysis. The data was finally exported into Excel spreadsheets for further analysis.

3.16 Reference Gene Stability

The stability of the reference genes was evaluated using the web-based tool RefFinder (https://blooge.cn/RefFinder/) which runs four well-established algorithms (GeNorm, BestKeeper, NormFinder and comparative delta-CT) to simultaneously compare and rank the three candidate reference genes (from most to least stable).

3.17 Total protein Extraction from FFPE Tissues of Patient Samples

This section covers the extraction of proteins using various methods. The purpose of exploring different methods was to determine which method would give the best protein yield. The methods employed were taken from the Quick DNA/RNA FFPE kit protocol, with and without the use of acetone for protein purification, (Shi et al., 2006), and (Ikeda et al.,1988), with modifications. Protein extraction with the use of acetone for protein purification, (Shi et al., 2006) and (Ikeda et al., 1998)'s methods yielded very low protein results; therefore, they were not further explored, and their results were not reported. The protein extraction using the Quick DNA/RNA FFPE kit, without the use of acetone for protein purification, was the chosen method for protein extraction in this study, as it gave the best protein yield.

3.17.1 Protein extraction method without acetone protein purification, using the Quick-DNA/RNA™ FFPE kit

3.17.1.1 Materials

Standard materials as reported in section 3.5.1 for the total RNA extraction using the Quick DNA/RNA FFPE kit, were utilized in this method for protein extraction.

3.17.1.2 Method

After the flow-through containing the proteins was obtained from the RNA extraction method, 100 µl of protease cocktail inhibitor, mixed with cell lytic agent (1:100), was added to each sample, vortexed and stored at -80 ^{0}C until use in protein quantification and western blot assay.

3.18 Extraction of Proteins from HepG2 Cell Line:

This section details the culturing and protein extraction from the HepG2 cell line. This cell line was used because it was readily available, with the objective to determine the lowest concentration of protein required for SDS-page. This was to establish whether the protein concentrations obtained from the patient samples would be sufficient for a successful western blot run. The method utilized was from Sigma-Aldrich (Catalog number: C2978).

3.18.1 Materials

TPP T75 tissue culture flasks (Sigma-Aldrich) for culturing of the cells; an inverted light microscope for viewing the confluency of the cells; a 5 % CO_2 incubator to foster the attachment and growth of the cells at 37 ^{0}C; DLab SK-0180-S (Biosmart scientific) for incubation of the cells following cell lytic treatment; a cell scraper (Thermofischer Scientific, SA) to remove cells from the plate to increase total protein yield; a centrifuge machine (Hermle); and a -80 ^{0}C freezer for storage of the protein sample.

The reagents used were: HepG2 cell line (Sigma-Aldrich, SA); Gibco Dulbecco's minimum essential media (DMEM) for growth of the cells (Thermofischer Life

technologies, SA); Gibco phosphate-buffered saline (PBS) pH 7.2 (Thermofischer Life technologies, SA) for washing of the cells; cell Lytic^{TM} M (Sigma-Aldrich, USA) for lysis and extraction of the proteins from the cells; and protease inhibitor cocktail (Sigma-Aldrich, USA) was used to prevent degradation of the proteins on extraction.

3.18.2 Method

Cells were defrosted at 37 °C and transferred from cryovials to culture flasks containing fresh, complete medium. The cells were grown in a humidified incubator set at 5 % CO2 until they reached 80-100 % confluence. After the cells had reached >80 % confluence, the medium was discarded, and the cells were washed with PBS. Protease inhibitor was diluted at 1:100 dilution in cell lytic agent, and 500 µl of that solution was added into the T75 flask and incubated for 15 minutes on a horizontal shaker. Thereafter, a cell scraper was used to remove some of the cells that were still adhering to the surface of the flask. The lysed cells were centrifuged for 15 minutes at 12,000-20,000 x g to pellet the cellular debris. Following this, the protein containing supernatant was removed, transferred into Eppendorf tubes, and stored in a -80 ^{0}C freezer until protein quantification.

3.19 Total Protein Quantification of Proteins

All the proteins extracted from different patients' samples using various methods and HepG2 cells were quantified with the Pierce BCA protein assay kit (Thermofischer Scientific, South Africa) to determine the best possible protein yields. The protocol utilized was from the Thermofischer BCA protein assay kit (Cat no. 23225 and 23227).

3.19.1 Materials

The following reagents were used during the BCA assay: Phosphate buffered saline was used as a diluent for the BSA standards. BCA reagent A, and BCA reagent B, were used to prepare the BCA working reagent. The BCA working reagents' objective was to react with Cu^{1+} ions of complexes between copper ions and peptide bonds to give rise to a

purple end product that absorbs strongly at 562 nm. The BCA working reagent (WR) was prepared by mixing 50 parts of BCA reagent A with 1 part of BCA reagent B. The total volume of BCA working reagent required was calculated using a formula stipulated in the protocol. (See the formula, below.) The BSA standard (2 mg/ml) was utilized, since it is the preferred standard in protein assays, and also due to its capacity to elevate signal in assays. The latter three solvents formed part of the BCA assay kit purchased from Thermofischer Scientific, South Africa. Foil was also used to cover the plates, as the BCA working reagent is light-sensitive.

Formula: *(no. of standards + no. of samples) x (no. of replicates) x (0.2 ml) = WR required)*

The 0.2 ml (200 µl) is the working reagent required for each well in the 96 microwell plates, based on the number of samples and replicates.

3.19.2 BCA protein assay method

A 2 mg/ml BSA standard stock solution was used. From the stock solution different concentrations were prepared, ranging from 2000 µg/ml – 25 µg/ml. Thereafter, 25 µl of each standard and protein sample were pipetted into individual wells on 96 well plates. For the blank, 25 µl of the diluent (PBS) was pipetted into the wells. Then, 200 µl BCA working reagent was added to the wells containing the standards, protein samples, and the blank. The plates were covered with foil and placed on the orbital shaker for 30 seconds to mix. After mixing, the plates were incubated at 37 ^{0}C for 30 minutes and then cooled to room temperature. Following this, the absorbance of the plates was read at 560 nm. The experiment was performed in duplicate. To obtain the corrected absorbances, the absorbance of the blank was subtracted from the absorbance measurements of all the other standards and protein samples. The corrected absorbance values were then plotted on GraphPad prism software to obtain a standard curve. Using the standard curve, the recorded, corrected absorbance readings for the samples assayed, which fell within the linear range of the standard curve, were then interpolated to obtain concentrations of the protein samples.

3.20 Imperial Staining (Protein Staining)

This section covers the staining of proteins extracted from the patient samples and HepG2 cells. This assay utilizes coomasie R-250 dye-based reagent for protein staining in polyacrylamide gels. Its sensitivity is such that it can stain proteins which are ≤3 ng. The bands can be viewed directly in the gel during the staining process. The protocol utilized was from Thermofischer Scientific.

3.20.1 Materials

Standard materials for measuring and aliquoting were used. Ice was used to keep the protein samples cold, and also during the running of the gel. Mini-protean TGX precast gels 10 % (w/v) (Bio-Rad, USA) were used. The mini-protean tetra system, and power-pac basic (Bio-Rad, USA) were used for the SDS-page. Mini-protean gel releasers were utilized to remove the gels from the cassette after the SDS-page run. The digital heat block (Benchmark, USA) was used to heat the protein samples prior to loading in the wells of the gel cassette. A Gilson (GV Lab, Germany) vortex machine was used to mix the samples, and the DLab SK-0180-S shaker was used during the washing and staining steps. Lastly, the Chemidoc imaging system (Bio-Rad, USA) was used for viewing the bands following the staining process.

The following reagents were used during the imperial protein staining assay: 10 x Tris/Glycine/SDS buffer (Bio-Rad, USA), and distilled water from the Elga Purelab chorus machine were used in the preparation of the running buffer during the SDS-page run. 2-Mercaptoethanol (Bio-Rad, USA), and 2x laemmli buffer (Bio-Rad, USA) were mixed in a 1:1 ratio and used as the loading buffer which was added to the protein samples. The precision plus protein western C standard (Bio-Rad, USA) was used as the molecular weight marker. Imperial protein stain (Thermofishcer Scientific, SA) was used to stain the SDS-page gels. Ultrapure deionized water was used during the washing of the gels.

3.20.2 SDS-PAGE gel electrophoresis

An aliquot of 14 µl per protein sample was mixed with 14 µl of the laemmli's sample buffer in Eppendorf tubes, which makes up 28 µl. This was the required volume for the loading of the protein samples in the gel, according to the protocol utilized for western blot assay. The concentrations of the patients' protein samples obtained in the BCA assay were used as is – they were not standardized. This was done to prevent over-diluting the protein samples. Following mixing of the proteins with the laemmli buffer, the samples were heated at 100 ^{0}C for 1 minute on the heat block. The SDS-page gels were assembled into the electrode assembly of the mini-protean tetra system, with the short plates facing inwards. The gel cassettes were then placed in the SDS-page tank and the inner chamber filled with 1x SDS-page running buffer. Thereafter, the gel combs were carefully removed from the gel, the molecular weight marker, and the protein samples, were added to the wells of the gel: 5 µl of the molecular weight marker was loaded in the first lanes of the gel, and 28 µl of the protein samples, mixed with the loading buffer, were added to the respective lanes of the gel. Once all the samples were loaded onto the gel, the inner chamber was topped up with the 1x SDS-page running buffer. Thereafter, the outer chamber was filled with an appropriate amount of cold 1x SDS-page running buffer, depending on the number of gels that were run (2 gels or 4 gels). The outside chamber marking was used as a guide for the amount of buffer to be used. Thereafter, the SDS-page tank (mini-protean tetra system) was closed with a lid, and it was placed in a glass dish filled with ice and connected to the powerpac. The SDS-page gel electrophoresis was run at 120 V for 2.5 hours.

3.20.3 Staining process

Following electrophoresis, the gels were removed from the cassettes using the gel releasers, placed in clean demarcated containers, and washed three times for 5 minutes, using 100 ml of ultrapure water. After the washing, a sufficient volume of the staining solution was added to each container to completely cover the gels. In this case, based on the dimensions of the container, 30 ml was added to each container, and the containers were placed on the shaker for staining for 2 hours. Once the 2 hours had elapsed, the staining reagent from each container was discarded and replaced with 200 ml of ultrapure

water per container and incubated on an orbital shaker overnight to reduce background colour and achieve the desired level of sensitivity. Following the overnight washing step, the gels were transferred to the Chemidoc imaging system to view the protein bands.

3.21 Statistical Analysis

Data was expressed as means ± SD. One-way anova was used to assess differences between the tumour and normal sections of patient samples in the poor vs. good responder groups. A $P<0.05$ was considered indicative of a statistically significant difference. Additionally, simple linear regression was used to interpolate unknowns from a linear standard curve of the BSA standard to obtain protein concentrations. A $P<0.001$ was considered statistically significant. All statistical analysis and graphs were generated with Graphpad Prism 10.0.2 (GraphPad software, Boston, USA).

CHAPTER 4:

RESULTS

4.1 RNA extraction

FFPE tissue samples from nine patients, separated into good and poor responders, were used to obtain RNA. Two sections, one labelled tumour (T) and the other normal (N), were removed from each patient's FFPE tissue block. RNA was extracted using the Zymoresearch Quick DNA/RNA FFPE kit. The RNA volumes extracted from the tissue sections of each subject are shown in Table 6, below. Following the protocol, 50 µl of RNA volume should be eluted from the column, for each tissue section from the patient samples. According to Table 6, below, most of the patient samples in the categories of good and poor responders had an RNA volume of 50 µl. The rest of the patient samples had RNA volumes of 40 to 45 µl.

Table 6: Eluted RNA volumes from patient samples in the different categories. (T) in the barcode denotes tumour section and (N) the normal cells section.

Good Responders				
Sample Name	**Sample no.**	**Sample Type (E.g) DNA/RNA**	**Origin**	**Sample Volume (µl)**
HS/16-8879	5T	RNA	Human FFPE Pca tissue biopsies	50
HS/16-8879	5N	RNA	Human FFPE Pca tissue biopsies	50
HS/19-1158	15T	RNA	Human FFPE Pca tissue biopsies	50
HS/19-1158	15N	RNA	Human FFPE Pca tissue biopsies	50
HS/21-2103	16T	RNA	Human FFPE Pca tissue biopsies	50
HS/21-2103	16N	RNA	Human FFPE Pca tissue biopsies	50
HS/18-7520	20T	RNA	Human FFPE Pca tissue biopsies	45
HS/18-7520	20N	RNA	Human FFPE Pca tissue biopsies	50
Poor Responders				
HS/16-15167	4T	RNA	Human FFPE Pca tissue biopsies	40
HS/16-15167	4N	RNA	Human FFPE Pca tissue biopsies	50
HS/16-2331	7T	RNA	Human FFPE Pca tissue biopsies	45
HS/16-2331	7N	RNA	Human FFPE Pca tissue biopsies	45
HS/21-1773	13T	RNA	Human FFPE Pca tissue biopsies	45
HS/21-1773	13N	RNA	Human FFPE Pca tissue biopsies	40
HS/18-13038	17T	RNA	Human FFPE Pca tissue biopsies	45
HS/18-13038	17N	RNA	Human FFPE Pca tissue biopsies	50
HS/19-11900	18T	RNA	Human FFPE Pca tissue biopsies	50
HS/19-11900	18N	RNA	Human FFPE Pca tissue biopsies	45

4.2 RNA Quantity and Quality

Data on the RNA quantity (concentrations) and quality (A260/A280 and A260/A230 ratios, RIN, DV200) are represented in Table 7. All samples had DV200 > 30% which suggests that the RNA could be used for real-time PCR.

An absorbance ratio of less than 1.8 indicates co-purification with impurities. This meant that they would interfere with downstream enzymatic reactions. At A_{260}/A_{280} the absorbances of most patients in the good and poor responder categories were all above 1.8.

Table 7: Total RNA quantity and quality. (T) marks tumour section, (N) marks normal section. OOR - out of range, this sample could not be quantified.

Good Responders						
Sample name	**Barcode**	**Nanodrop RNA concentration (ng/µl)**	**Qubit RNA concentration (ng/µl)**	**A260/280**	**A260/230**	**DV200 (%)**
HS/16-8879	5T	39,24	43,20	1,76	1,37	57.03
HS/16-8879	5N	39,16	6,69	1,9	0,23	68.58
HS/19-1158	15T	76,88	100,00	2,01	1,31	59.35
HS/19-1158	15N	37,16	37,40	1,88	1,13	60.54
HS/21-2103	16T	43,8	62,00	1,88	1,41	61.69
HS/21-2103	16N	18,92	19,60	1,79	0,22	57.63
HS/18-7520	20T	39,96	46,70	2,01	1,48	57.55
HS/18-7520	20N	35,72	13,40	1,56	0,48	48.49
Poor Responders						
HS/16-15167	4T	1,08	OOR	2,42	0,03	46.87
HS/16-15167	4N	12,84	10,40	1,66	0,23	61.17
HS/16-2331	7T	22,68	32,10	2,2	0,52	52.67
HS/16-2331	7N	31,8	37,20	1,95	0,34	47.78
HS/21-1773	13T	52,16	78,00	1,98	0,85	63.70
HS/21-1773	13N	84,52	76,00	2,04	1,32	60.67
HS/18-13038	17T	14,68	12,80	1,86	0,77	50.45
HS/18-13038	17N	23,96	14,50	1,76	0,33	65.54
HS/19-11900	18T	25,6	14,10	1,71	0,95	51.40
HS/19-11900	18N	10,72	7,80	1,54	0,03	55.49

The absolute RNA concentrations in the patient samples were calculated using the RNA Qubit kit. The RNA concentrations of the patients in the categories of good and poor responders are shown in Table 7. In the good responder category, the highest concentration of 100 ng/µL was measured (15T), while some samples (e.g 5N) yielded

the lowest concentration of 6.69 ng/µL. Furthermore, it was observed that all patient sample's tumour sections had higher RNA concentrations than their normal sections.

For the poor responder category, the highest concentration of 78 ng/µL was measured (13T), while some samples (e.g 18N) yielded the lowest concentration of 7.8 ng/µL. Samples 13T, 17T, and 18T's tumour sections had higher RNA quantities than their relative to their normal cell sections. The exception was patient sample 7N, which had a greater RNA concentration than its tumour section (7T). Lastly, sample 4T could not be compared to sample 4N since it was out of range and its RNA concentration could not be established.

Figure 9, below, provides a graphical illustration of the comparisons between the RNA concentrations of patients in the good versus poor responder categories of both the tumour and normal sections. The RNA concentrations of the sections in the good vs. poor responders' categories were not statistically significant, according to the one-way anova test.

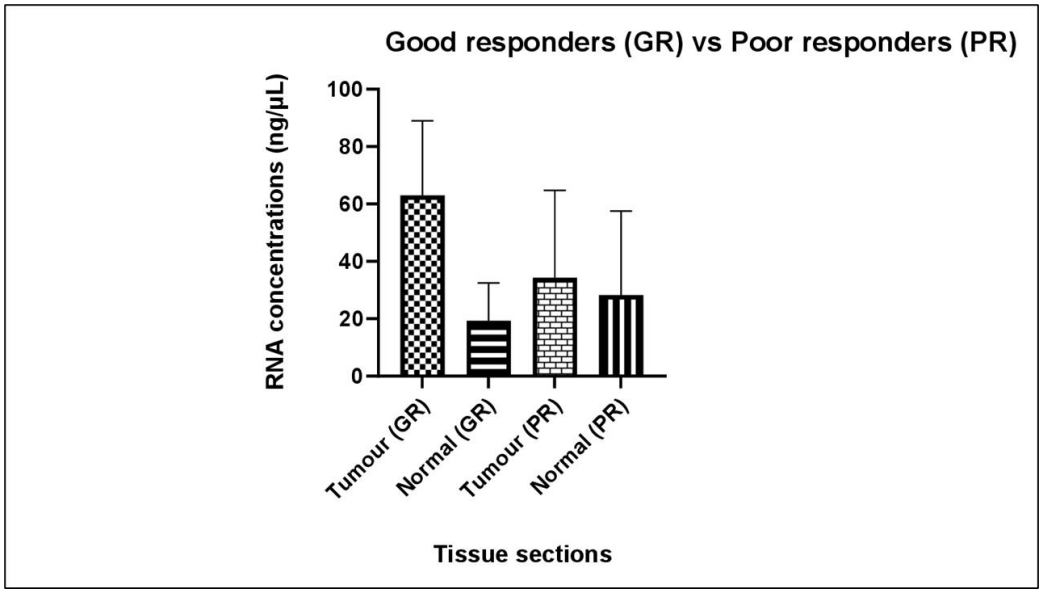

Figure 9: Comparisons of RNA concentrations between the tumour and normal sections of patients in the good vs poor responder categories. Statistical significance was tested by one-way anova. Tumour (GR) vs Tumour (PR), p=0.431. Normal (GR) vs Normal (PR), p=0.954

4.3 RNA Integrity

The RNA samples were examined using the RNA Tapestation's RNA ScreenTape and high sensitivity RNA Screentape to ascertain their integrity. Table 8 shows the RNA integrity numbers (RIN) of the patients in the categories of good and poor responders. In the good responder category, sample 20N had the highest RIN of 3.0; whereas sample 5N had the lowest RIN of 2.0. In the poor responder category, sample 17N had the greatest RIN of 3.8; while sample 13N had the lowest RIN of 1.7. Sample 4T's RNA concentration was outside the functional range for RIN measurement because its concentration was less than 0.2ng/µL.

Table 8: RINs of patients in the good and poor responder categories. (T) marks tumour section, (N) marks normal section. [-] - Sample concentration outside functional range for RIN measurement.

Good Responders		
Sample Name	**Barcode**	**RIN**
HS/16-8879	5T	2,20
HS/16-8879	5N	2,00
HS/19-1158	15T	2,60
HS/19-1158	15N	2,40
HS/21-2103	16T	2,10
HS/21-2103	16N	2,10
HS/18-7520	20T	2,90
HS/18-7520	20N	3,00
Poor Responders		
Sample Name	**Barcode**	**RIN**
HS/16-15167	4T	[-]
HS/16-15167	4N	2,30
HS/16-2331	7T	2,40
HS/16-2331	7N	2,10
HS/21-1773	13T	2,00
HS/21-1773	13N	1,70
HS/18-13038	17T	3,10
HS/18-13038	17N	3,80
HS/19-11900	18T	3
HS/19-11900	18N	3,1

4.4 SPUD Inhibition Assay

The SPUD qPCR inhibition assay was used for the detection of potential qPCR inhibitors in the FFPE RNA samples. All RNA samples recorded Cq values within a 0.09 cycle of the negative control and were thus considered to be free of inhibitors affecting the SPUD assay. Table 9, below, displays the SPUD assay results of patient samples in the good and poor responder categories.

Table 9: Assessment of RT-qPCR inhibition in the FFPE RNA samples.

Good Responders				
Sample name	**Barcode**	**Cq mean**	**∆Cq (Cq Sample – Cq Control)**	**Inhibition indicated**
HS/16-8879	5T	21,85	0,03	No
HS/16-8879	5N	22,2	0,4	No
HS/19-1158	15T	21,8	0,08	No
HS/19-1158	15N	21,71	-0,01	No
HS/21-2103	16T	21,79	0,01	No
HS/21-2103	16N	21,77	-0,03	No
HS/18-7520	20T	21,75	-0,14	No
HS/18-7520	20N	21,89	0,02	No
Poor Responders				
HS/16-15167	4T	21,81	0,07	No
HS/16-15167	4N	21,73	0,09	No
HS/16-2331	7T	21,82	-0,03	No
HS/16-2331	7N	21,85	0,08	No
HS/21-1773	13T	21,72	-0,09	No
HS/21-1773	13N	21,82	-0,01	No
HS/18-13038	17T	21,74	0,03	No
HS/18-13038	17N	21,7	-0,08	No
HS/19-11900	18T	21,87	0,04	No
HS/19-11900	18N	21,83	0,09	No

4.5 5’-3’ Integrity Assay

All the FFPE RNA samples recorded 3’Cq values between 22,4 and 30,1, and the 5’Cq was very high (28,6 – 32,5), resulting in high ∆Cq5'-3' values (Table 10). Subsequently, the 5’Cq’s were below detection level for half the samples and as a result the ∆Cq5'-3' could not be calculated.

Table 10: Results of the 5'-3' Integrity Assay. UND – undetermined (the 5’ Cq was below detection level). NC – the ∆Cq5'-3' could not be calculated. HeLa RNA was included as a positive control for the cDNA synthesis kit. XpressRef universal RNA was included as a positive control for intact RNA samples.

Good Responders				
Sample	**Barcode**	**Cq5'GAPDH**	**Cq3'GAPDH**	**∆Cq5'-3'**
HS/16-8879	5T	31,6	22,4	9,2
HS/16-8879	5N	UND	28,3	NC
HS/19-1158	15T	30,5	23,8	6,7
HS/19-1158	15N	32,2	24,5	7,6
HS/21-2103	16T	UND	23	NC
HS/21-2103	16N	UND	24,4	NC
HS/18-7520	20T	31,8	25,7	6,1
HS/18-7520	20N	32	28	4
Poor Responders				
HS/16-15167	4T			
HS/16-15167	4N	UND	30,1	NC
HS/16-2331	7T	UND	25	NC
HS/16-2331	7N	32,4	24,3	8,1
HS/21-1773	13T	29,8	21,5	8,3
HS/21-1773	13N	28,6	20,9	7,7
HS/18-13038	17T	UND	28	NC
HS/18-13038	17N	UND	28,4	NC
HS/19-11900	18T	UND	29,8	NC
HS/19-11900	18N	UND	29	NC
HeLa		22,6	21,1	1,6
XpressRef Universal RNA		20,5	19,6	1

4.6 qPCR Primers

The qPCR primers used for the project (Table 11) were designed using Primer-BLAST, selected from the literature, or sourced from PrimerBank. Primer-BLAST primer design parameters are shown in Table 12.

Table 11: Primer nucleotide sequences and product lengths for the target and reference genes amplification by qPCR.

Gene Symbol	Primer name	Primer sequence (5' -----3')	Amplicon size	Reference
ABCC1	3-abcc1Fp1	AGC CCA AAG TGG AAT CCG GAA G		
	3-abcc1Rp1	AGT CGG CGG CGT AAT TCT TAG C	80 bp	This study
ABCC2	ABCC2pp4F	AGGCTGCACACCATCATGGAC		
	ABCC2pp4R	TCTCAATGCCAGCTTCCTTAGCC	136 bp	This study
ABCC10	ABCC10pp1F	CGGCCTGCTCTATGCTCTG		
	ABCC10pp1R	CCCCGTGCCTGAAGTGTTA	105 bp	PrimerBank ID 312176402c3
GAPDH	3-GAPDHFp	AGT CCC TGC CAC ACT CAG		
	3-GAPDHRp	TAC TTT ATT GAT GGT ACA TGA CAA	123 bp	Nolan et al. 2006
HPRT1	HPRT1F	GAC CAG TCA ACA GGG GAC AT		
	HPRT1R	CCT GAC CAA GGA AAG CAA AG	132 bp	Liu et al. 2015
HSPCB	HSPCBF	TCT GGG TAT CGG AAA GCA AGC C		
	HSPCBR	GTG CAC TTC CTC AGG CAT CTT G	80 bp	Jacob et al. 2013

Table 12: Primer-BLAST primer design selection criteria.

Primer Design Criteria	Selected Parameters
Primer Location	3'- end
PCR product size (bp)	Min = 80 Max = 200
Primer Tm (°C)	Min = 60 Opt = 63 Max = 65
Max. Tm difference [°C] between the primers	1
Primer size (nucleotides)	Min = 18 Opt = 21 Max = 24
Primer GC content (%)	Min = 40 Max = 60
GC clamp	1
Max Poly-X	3
Max GC in primer 3' end	3
SNP handling	Primer binding site may not contain known SNP
Intron inclusion	Primer separated by at least one intron on the corresponding genomic DNA
Intron length range	Min = 200

4.7 qPCR Assay Optimization and Validation

4.7.1 Standard Curves – calculation of PCR efficiency to measure assay performance

The PCR efficiency (linearity of amplification) of the qPCR assays was assessed by generating a standard curve using two-fold and ten-fold dilution series of the universal cDNA template. The Cq values obtained at each dilution were then plotted against the log of the cDNA dilution and the amplification efficiency E calculated from the slope of the standard curve using the equation E = (10- 1/slope)-1, where E is PCR efficiency. The ideal efficiency is 100% (slope = -3.3), but an efficiency in the range of 90 – 110% (slope between -3.5 and -3.2) is acceptable, according to the MIQE guidelines (Bustin et al., 2009). The qPCR primers used in the project showed qPCR efficiencies within the acceptable range and with high linearity (R2 ≥ 0.99), except for ABCC10 (E = 117.96%).

4.7.2 Assay specificity

Specificity of each assay during the optimizations was verified using non-reverse transcribed RNA (NRT) and no template control (NTCs), and assay specificity was validated by melt curve analysis. No amplification was seen with NRT and NTC. All qPCR assays showed amplification of single amplicons as shown by single Tm peaks on melt curves (Figures 10.1(A-F) and 10.2 (G-L)).

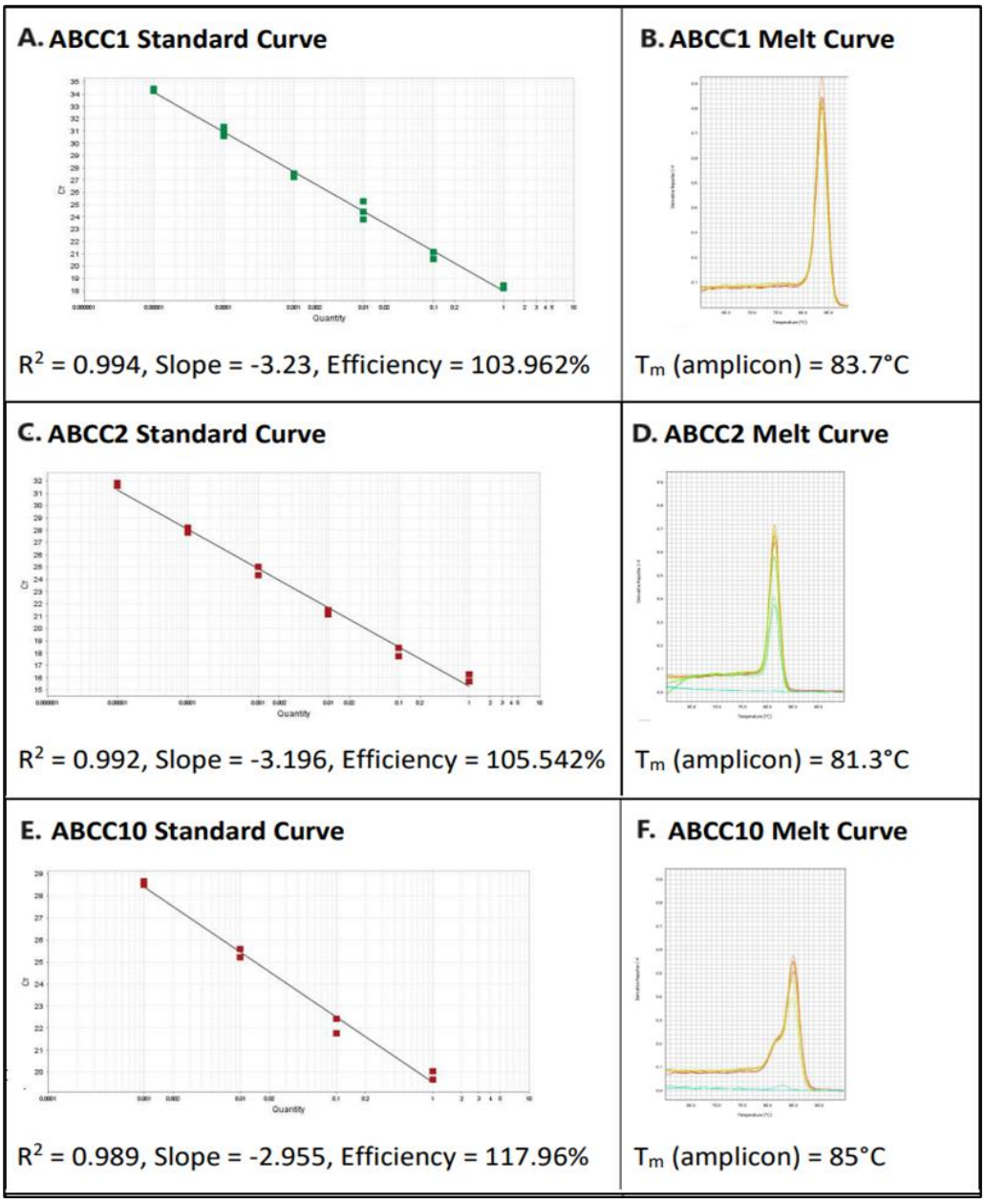

Figure 10.1 (A-F): Determination of qPCR efficiencies of target genes (ABCC1, ABCC2, ABCC10). Standard curves (on the left) using two-fold dilution series of the XpressRef Universal cDNA for ABCC1 (A) and ten-fold dilution series for the rest of the amplicons. CT (Cq) cycles versus log cDNA concentration input were plotted to calculate the slope. The corresponding qPCR efficiencies were calculated using to the equation: E = 10(-1/slope). Melt curve plots (on the right) of qPCR assays show a single Tm peak for a specific amplicon in each assay. Tm of each amplicon of each assay are shown.

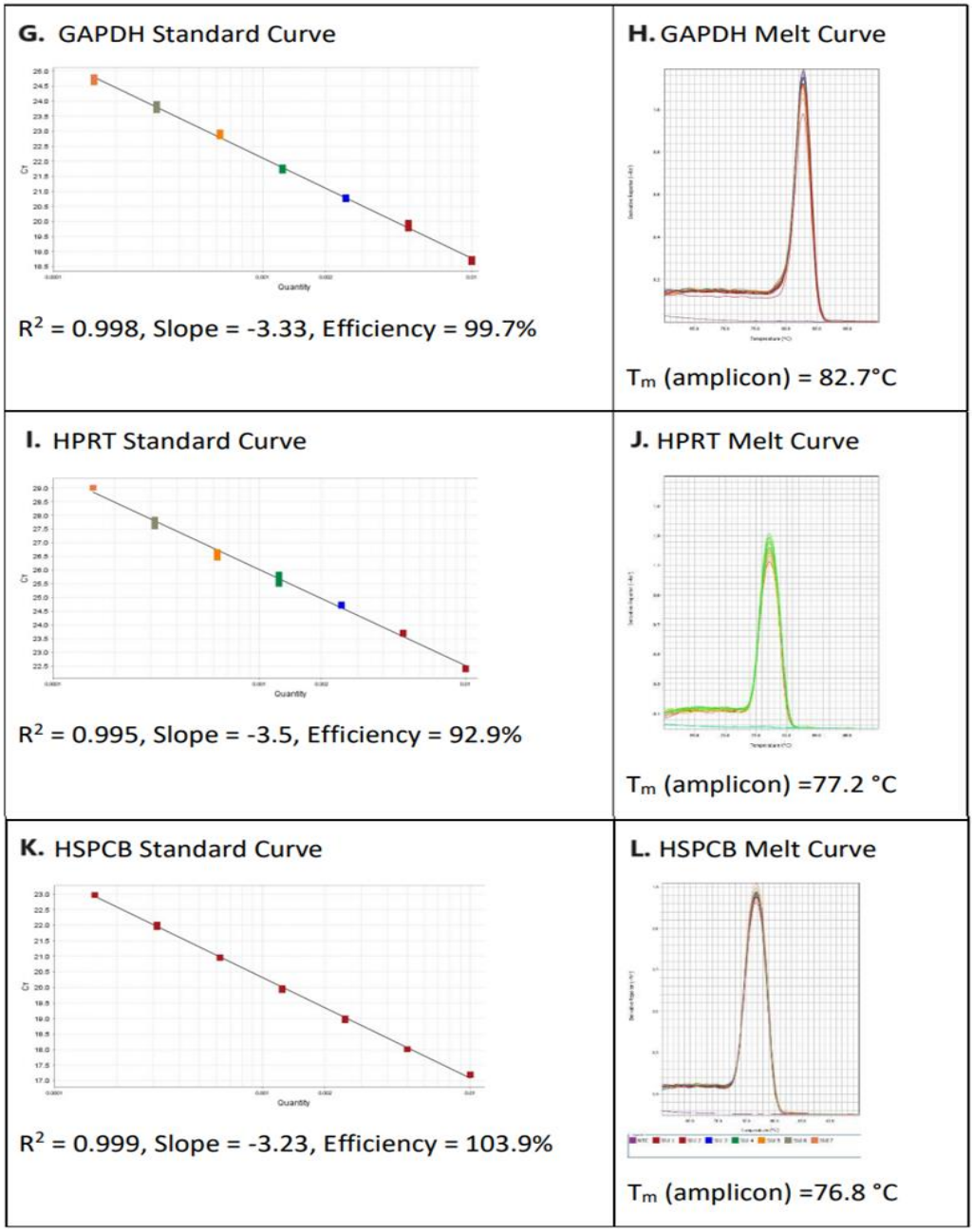

Figure 10.2 (G-L): Determination of qPCR efficiencies of reference genes (GAPDH, HPRT, HSPCB). Standard curves (on the left) using two-fold dilution series of the XpressRef Universal cDNA for ABCC1 (A) and ten-fold dilution series for the rest of the amplicons. CT (Cq) cycles versus log cDNA concentration input were plotted to calculate the slope. The corresponding qPCR efficiencies were calculated using to the equation: E = 10(-1/slope). Melt curve plots (on the right) of qPCR assays show a single Tm peak for a specific amplicon in each assay. Tm of each amplicon of each assay are shown.

4.8 qPCR

Expression values (Cq) of each target and reference gene were collected and sorted according to biological groups (normal vs tumour). These are shown in Table 13.

Table 13: Mean Cq values (of three replicates) for each target and reference gene using preamplified cDNA samples as templates for qPCR. UND, Cq value un-determined. Positive control sample: XpressRef universal total RNA (QIAGEN) for gene expression.

Good Responders							
Sample Name	**Biological Group**	**Cq^{ABCC1}**	**Cq^{ABCC2}**	**Cq^{ABCC10}**	**Cq^{GAPDH}**	**Cq^{HPRT}**	**Cq^{HSPCB}**
5T	Tumour	22,0	33,18	23,54	17,4	26,3	19,6
5N	Normal	21,6	28,09	23,68	17,6	UND	19,8
15T	Tumour	22,3	26,86	23,13	19	UND	18,9
15N	Normal	21,8	26,13	23,2	18,1	28,2	18,3
16T	Tumour	21,8	27,52	22,28	16,9	32,6	18,8
16N	Normal	21,8	28,15	22,55	16,7	27,3	18,8
20T	Tumour	23,5	30,88	23,39	19,6	31,6	20,1
20N	Normal	24,5	30,9	23,82	20,70	24,80	21,0
Poor Responders							
4T	Tumour	29,3	UND	28,25	25,9	26,8	27,2
4N	Normal	23,9	UND	25,13	21,4	33,8	22,4
7T	Tumour	22	29,85	24,53	18,5	UND	20
7N	Normal	21,9	28,66	23,71	17,8	27,7	19,7
13T	Tumour	21,4	27,33	21,61	15,9	29,7	17,4
13N	Normal	21,0	27,24	21,7	15,6	UND	17,3
17T	Tumour	23,1	UND	24,31	20,3	29,9	20,9
17N	Normal	23,6	31,14	25,78	24,2	27,8	22,8
18T	Tumour	25,2	UND	24,53	22,2	28,4	23,2
18N	Normal	29,5	UND	32,33	29,1	25,4	26,5
CTRL	Control sample	21	18,08	21,71	14,1	22,1	14,8

4.9 Reference Gene Selection - Evaluation of the Stability of the Reference Genes

HSPCB was ranked the most stable of the three genes by all the RefFinder algorithms, followed by GAPDH (Table 14). Both HSPCB and GAPDH are recommended for normalization of the Cq values of the target genes during relative quantitative data analysis.

Table 14: Ranking and stability values of the three reference genes. The rank order (1-3) for each gene is shown for each algorithm (in parenthesis). The overall rank order of the reference genes is shown.

Reference Gene Stability			
Algorithm	**HSPCB**	**GAPDH**	**HPRT**
ΔCT	1	2	3
BestKeeper	1	2	3
NormFinder	1	2	3
GeNorm	1	1	3
Overal Rank	**1**	**2**	**3**

4.10 Relative Expression Levels of ABCC1/MRP1, ABCC2/MRP2, and ABCC10/MRP7

Table 15, below, shows the expression levels of ABC-transporter genes. In the good responders' category, the average expression levels of ABCC1, ABCC2, and ABCC10 were 20-50-fold higher in the normal sections, than in the tumour sections of the patient samples. The results suggest that MRP1, MRP2 and MRP7 were highly expressed in the normal sections than in the tumour sections. Overall, ABCC2/MRP2 was the most highly expressed in both the tumour and normal sections of the patients. Moreover, sample 20N showed the highest expression of all three genes, compared to the other samples. For the poor responders' category, the average expression levels of ABCC1/MRP1 and ABCC10/MRP7 were 3-5-fold higher in the tumour sections, than in the normal sections of the patient samples. This suggests that MRP1 and MRP7 were highly expressed in the tumour sections. In general, ABCC10/MRP7 was the most highly expressed in both the tumour and normal sections of the patients' samples.

In comparing the good responders' category to the poor responders' category, the expression levels of ABCC1 and ABCC10 in the tumour sections were 2-4-fold lower, than in the tumour sections of the poor responders' category. Subsequently, the average expression levels of ABCC1 and ABCC10 in the normal sections of the good responders' category, were 40-60-fold higher than in the normal sections of the poor responders' category. The expression levels of ABCC2 could not be determined in about half the patient samples in the poor responders' category, therefore, an adequate comparison could not be drawn between the tissue sections in the two categories, in terms of the average expression levels of ABCC2.

Table 15: Relative expression levels of ABCC1, ABCC2, and ABCC10 in the good and poor responder categories. (T) indicates tumour, and (N) indicates normal sections.

Expression Levels				
Good Responders				
Sample Name	**Barcode**	**ABCC1**	**ABCC2**	**ABCC10**
HS/16-8879	5T	0,438	4,385	0,642
HS/16-8879	5N	0,865	0,063	0,660
HS/19-1158	15T	0,379	0,812	1,340
HS/19-1158	15N	0,362	0,870	0,654
HS/21-2103	16T	0,340	0,136	1,235
HS/21-2103	16N	0,324	0,023	0,953
HS/18-7520	20T	0,000	4,188	3,109
HS/18-7520	20N	61,066	364,865	152,233
Poor Responders				
Sample Name	**Barcode**	**ABCC1**	**ABCC2**	**ABCC10**
HS/16-15167	4T	1,009		0,341
HS/16-15167	4N	0,184		0,019
HS/16-2331	7T	0,841	0,605	0,204
HS/16-2331	7N	0,586	0,000	0,627
HS/21-1773	13T	0,238	0,091	0,907
HS/21-1773	13N	0,312	0,097	0,812
HS/18-13038	17T	2,420		15,674
HS/18-13038	17N	0,001	1,108	0,038
HS/19-11900	18T	0,909		0,171
HS/19-11900	18N	0,744		1,549

Figures 11, 12 and 13 provide graphical presentations of the expression levels of ABCC1, ABCC2, and ABCC10 in the samples of patients in the good vs. poor responder categories. Statistical significance was determined using one-way anova.

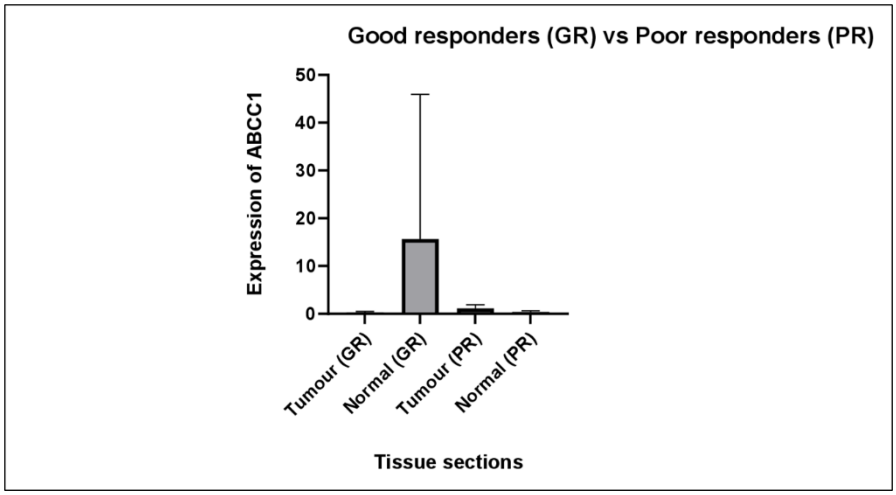

Figure 11: Comparison of ABCC1 expression levels in the (T) and (N) sections of patients in the good vs. poor responder categories. Statistical significance was tested by one-way anova. Tumour (GR) vs Tumour (PR), p>0,999. Normal (GR) vs Normal (PR), p=0.397. No statistical significance was observed.

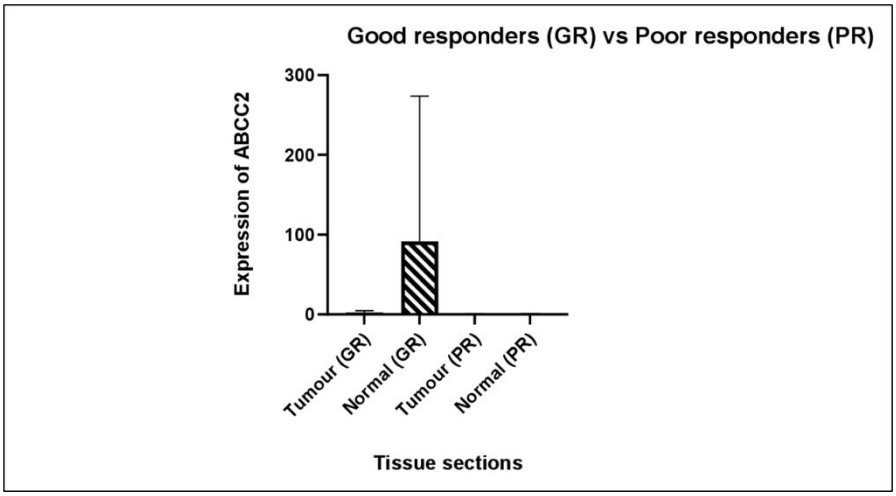

Figure 12: Comparison of ABCC2 expression levels in the (T) and (N) sections of patients in the good vs. poor responder categories. Statistical significance was tested by one-way anova. Tumour (GR) vs Tumour (PR), p>0,999. Normal (GR) vs Normal (PR), p=0.680

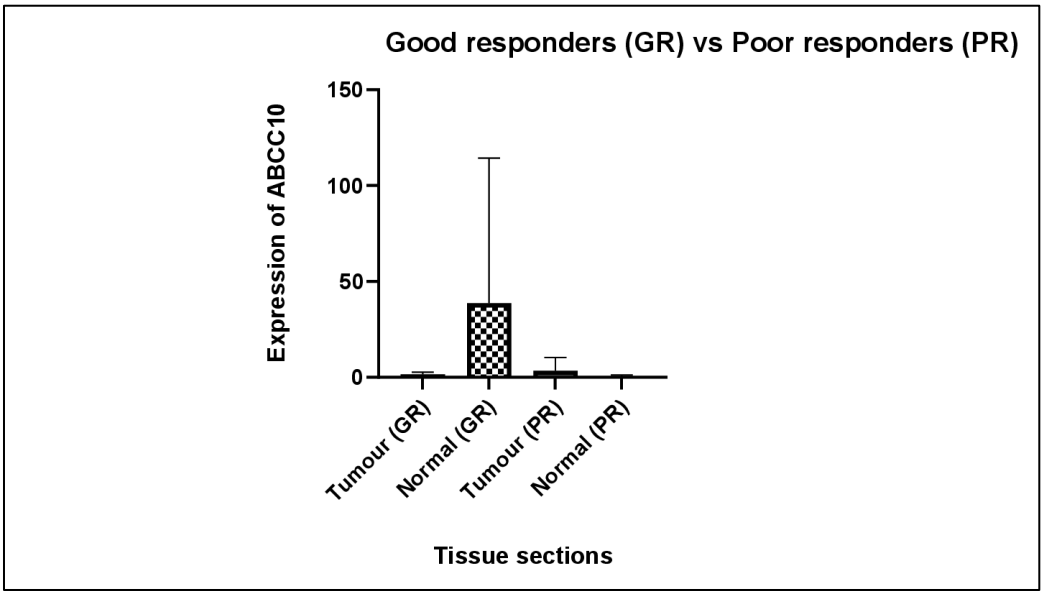

Figure 13: Comparison of ABCC10 expression levels in the (T) and (N) sections of patients in the good vs. poor responder categories. Statistical significance was tested by one-way anova. Tumour (GR) vs Tumour (PR), p>0.999. Normal (GR) vs Normal (PR), p=0.406. No statistical significance was observed.

4.11 Protein Quantification

4.11.1 Protein extraction <u>without</u> acetone protein purification

Table 16, below, shows the protein concentrations of patients in the good and poor responder categories, whose proteins were extracted using the protein extraction without-acetone method. Proteins were extracted from each excised section, from the patients' FFPE tissue blocks according to the category they fall under. In this method, the proteins were extracted using the Zymoresearch Quick DNA/RNA FFPE kit. After obtaining the protein-containing flow-through, it was not purified using cold acetone. To avoid degradation, only the inhibitor was introduced, and the samples were measured to provide the protein quantities represented in Table 16, below. Proteins that were extracted from all the patient samples utilised this method of extraction. This was because this approach, out of all the protein extraction methods investigated in the study, produced the highest protein yield.

In the good responder category, the protein concentrations of the patient samples were all above 100 µg/ml. Sample 20N had the highest protein concentration (340, 63 µg/ml), while sample 5N had the lowest protein concentration (149, 44 µg/ml). Furthermore, it was observed that for all the patient samples, except for 5T and 5N, all the normal tissue (N) sections had higher protein concentrations compared to their tumour sections (T). The opposite was observed for sample 5T, the tumour section had a higher protein concentration of 264,09 µg/ml in comparison to its control, the normal section (5N), which had a protein concentration of 149,44 µg/ml.

For the poor responder group, the highest protein concentration of 328,29 µg/ml was observed in sample 13T. The lowest protein concentration of 249,33 µg/ml was seen in sample 17N. Moreover, in this category, it was observed that in all the patient samples, except for patient sample 7T and 7N, the tumour sections (T) yielded higher protein concentrations in comparison to their normal sections (N). However, in the sections for patient sample 4T & 4N, the opposite was observed because the normal section (4N) had a higher protein concentration of 297,85 µg/ml, compared to the tumour section (4T) with a protein concentration of 256, 01 µg/ml.

The findings in the poor responder group are the opposite of the findings in the good responder group. From the patient samples in Table 16, of the good responder group, 87.5% had high protein concentrations in the normal sections (N); whereas 90% of the patient samples from the poor responder group, shown in Table 16, had high protein concentrations in the tumour sections (T).

.

Table 16: Protein concentrations of patients in the good and poor responder category. (T) represents tumour, and (N) represents normal section. R^2= 0.9981, p<0.001.

Good Responders			
Sample Name	**Barcode**	**Extraction method**	**Protein Concentration (µg/ml)**
HS/16-8879	5T	Zymoresearch DNA/RNA FFPE Kit	264,09
HS/16-8879	5N	Zymoresearch DNA/RNA FFPE Kit	149,44
HS/19-1158	15T	Zymoresearch DNA/RNA FFPE Kit	264,57
HS/19-1158	15N	Zymoresearch DNA/RNA FFPE Kit	293,13
HS/21-2103	16T	Zymoresearch DNA/RNA FFPE Kit	278,02
HS/21-2103	16N	Zymoresearch DNA/RNA FFPE Kit	327,95
HS/18-7520	20T	Zymoresearch DNA/RNA FFPE Kit	311,30
HS/18-7520	20N	Zymoresearch DNA/RNA FFPE Kit	340,63
Poor Responders			
Sample Name	**Barcode**	**Extraction method**	**Protein Concentration (µg/ml)**
HS/16-15167	4T	Zymoresearch DNA/RNA FFPE Kit	256,01
HS/16-15167	4N	Zymoresearch DNA/RNA FFPE Kit	297,85
HS/16-2331	7T	Zymoresearch DNA/RNA FFPE Kit	274,08
HS/16-2331	7N	Zymoresearch DNA/RNA FFPE Kit	268,37
HS/21-1773	13T	Zymoresearch DNA/RNA FFPE Kit	328,29
HS/21-1773	13N	Zymoresearch DNA/RNA FFPE Kit	281,66
HS/18-13038	17T	Zymoresearch DNA/RNA FFPE Kit	263,60
HS/18-13038	17N	Zymoresearch DNA/RNA FFPE Kit	249,33
HS/19-11900	18T	Zymoresearch DNA/RNA FFPE Kit	325,40
HS/19-11900	18N	Zymoresearch DNA/RNA FFPE Kit	250,29

Figure 14, below, is a graphical representation of the protein concentrations in the (T) and (N) sections of patients in the good vs poor responder categories. Statistical analysis was determined using the one-way anova. No statistical significance was observed between the categories.

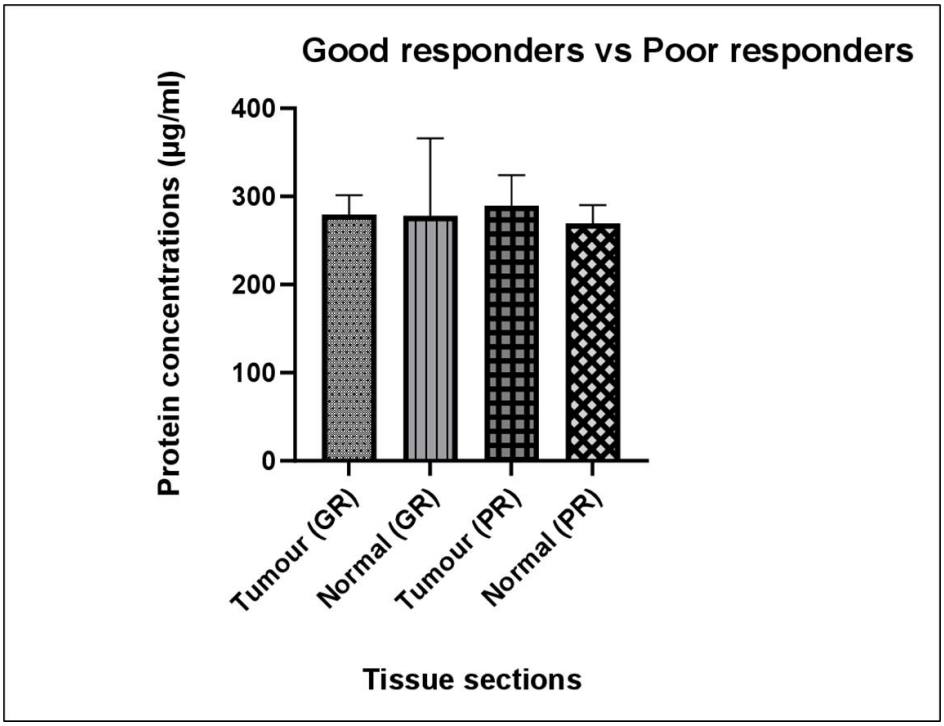

Figure 14: Comparison of protein concentrations in the (T) and (N) sections of patients in the good vs. poor responder categories. Tumour (GR) vs. Tumour (PR), p=0.989. Normal (GR) vs Normal (PR), p=0.993

4.12 HepG2 Cells' Protein Concentration

Following protein extraction, western blot analysis was performed. The results however, showed no protein bands. Possible explanations included low protein concentration. To troubleshoot, HepG2 cells were cultured for the purpose of obtaining sufficient amounts of protein to run on a gel. The HepG2 cells' proteins were extracted utilising the CelLytic™ reagent. The extracted proteins were quantified using the same BCA assay method as the other proteins in the study. The obtained protein concentration was used to prepare half dilutions ranging from 500 µg/ml to 15,625 µg/ml. These concentrations were used

for loading in the SDS-page required for the imperial staining assay, to detect proteins. Table 17, below, shows the protein concentration of HepG2 cells (665.28 µg/ml) obtained from >80% confluent flask.

Table 17: Protein concentration of HepG2 cells. R^2=0.9930, p<0.001.

HepG2 cell line		
Disease	**Extraction Method**	**Concentration (µg/ml)**
Hepatocellular carcinoma	CelLytic M reagent	665.28

4.13 Imperial Protein Staining

The imperial protein stain was carried out using protein samples from patients in the good and poor responder categories and proteins from HepG2 cells.

Three gels were run for the detection of proteins with the imperial protein stain. Gel 1 was loaded with protein samples from the good responders, with the exception of sample 4T which belongs to the poor responder's category. Gel 2 was loaded with protein samples from the poor responders. Lastly, Gel 3 was loaded with half dilutions of the protein concentration obtained from HepG2 cells, ranging from 500 µg/ml to 15,625 µg/ml. Figures 15 and 16 display the imperial stain of gel 1 and 2. No proteins (MRP1/ABCC1) were detected in any of the patient samples in the good responder category (Fig 15) and the poor responder category (Fig 16), while protein bands were observed in all lanes loaded with different protein concentrations of HepG2 cells (Fig 17). The expression of the bands decreased as the concentrations became lower.

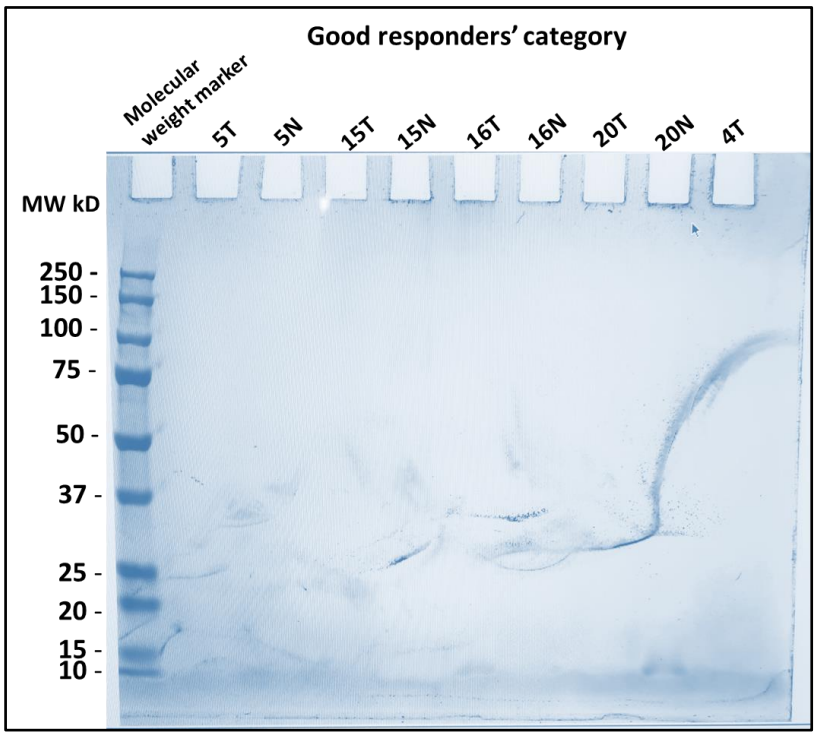

Figure 15: Imperial stain image of Gel 1, indicating the good responder's category protein expression, with the exception of lane 10, which represents a poor responder's sample (4T).

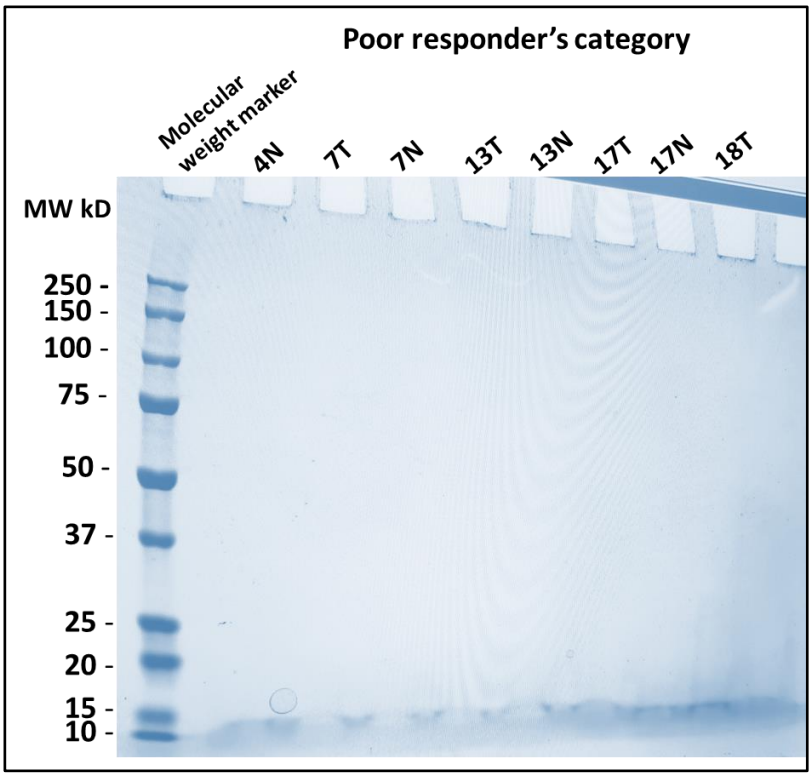

Figure 16: Imperial stain image of Gel 2 indicating the poor responder's category protein expression.

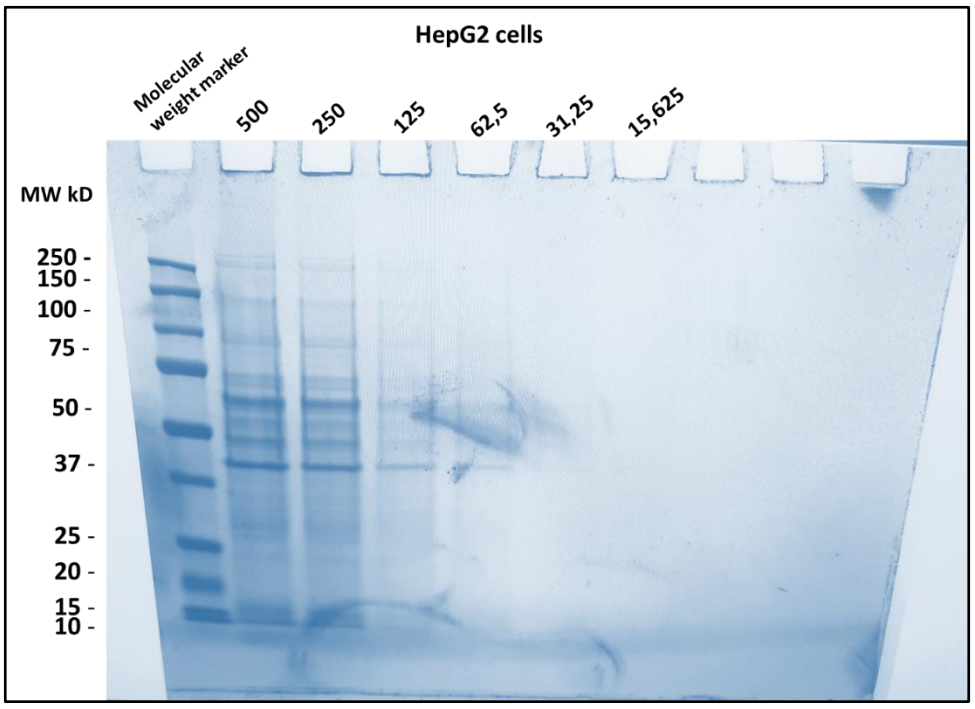

Figure 17: Imperial stain of Gel 3 indicating the HepG2 cells protein expression.

CHAPTER 5:

DISCUSSION

FFPE blocks archived at room temperature are more economical in terms of upkeep, space and labour, than storing frozen tissues at extremely low temperatures (Kokkat et al., 2013). Previous studies reported that there is no significant difference in RNA quality between frozen tissues and FFPE tissues (Choi et al., 2017). The large numbers of FFPE tissue samples archived in the pathology departments of hospitals, are a reliable resource for research material (Yi et al., 2020). Proteins and nucleic acids (RNA and DNA) can now be extracted from FFPE blocks and used in downstream applications, such as quantitative RT-PCR and western blot, because of developments in the field of molecular biology (Kokkat et al., 2013).

In this study, nine FFPE tissue blocks were obtained from the pathology department at NHLS and divided into two categories, good responders, and poor responders. The good responder category contained four patient samples (FFPE blocks) and the poor responders category contained five FFPE blocks. According to the literature pertaining to *in vivo* studies, a sample size of five animals per group is sufficient to provide credible results (Auta and Hassan, 2016, Kobeissy et al., 2017). Therefore, five samples per group is accepted and used widely in science. Concerns over statistical integrity, costs, and using the minimum samples necessary for proof of concept were considered. Therefore, the sample size selected for the two categories in this study was determined using guidance from *in vivo* peer reviewed studies as a point of reference (Auta and Hassan, 2016, Kobeissy et al., 2017).

RNA and proteins were extracted from the same tumour and normal (non-tumour) sections cut from each of these nine FFPE blocks. The FFPE blocks had been archived from one to six years. Total RNA was extracted in 50 µl of DNase/RNase-free water (see Table 6). The RNA volume extracted from the patient samples ranged from 40 to 50 µl. This volume was sufficient to carry out the RNA quantification, quality and purity assessment assays, because the RNA volumes that were required ranged from 1-20 µl, depending on the assay (Vermeulen et al., 2011) and (Thermofischer Invitrogen, Qubit RNA HS assay kit).

Following RNA extraction, the RNA was subjected to quantification and purity assessment (see Table 7). Total RNA purity was assessed using the NanoDrop 8000 instrument to determine the level of impurities, such as proteins (A260/280 value) and polysaccharides, polyphenols and chaotropic salts (A260/230 value).

An absorbance ratio less than 1.8 indicated co-purification with impurities, which would interfere with downstream enzymatic reactions. Most of the patient samples had an RNA purity of between 1.8 and 2.42, indicating a high level of purity. Furthermore, the RNA extracted from the patient samples had a DV200>30%, which suggested that the RNA could be utilised for quantitative RT-PCR. The results presented in Table 7 for the RNA purity assessment are consistent with those of (Kokkat et al., 2013) who reported values between 1.95 and 2.18 at A260/280, although they were focusing on RNA extracted from FFPE blocks of different cancers (malignant lung, thyroid and salivary gland). Additionally, these results are also consistent with a study published by Yi et al (2020), who reported RNA purity of 2.0 ± 0.1 at A260/280, and one by Choi et al (2017), who reported RNA purity of between 1.78 and 2.04. Also, Table 7 shows the RNA concentrations obtained from the patient samples using the Qubit RNA HS assay kit. Most patient samples in both the good and poor responder categories had RNA concentrations above 10 ng/µL; except for samples 5N (good responder) and 18N (poor responder), which had an RNA concentration lower than 10 ng/µL. An RNA concentration of 10 ng/µL indicates that the RNA is eligible for downstream applications (Yi et al., 2020).

It is stated that RNA integrity is crucial for obtaining trustworthy results (Vermeulen et al., 2011). Inadequate sample handling, extended storage, unsuitable storage conditions, or sample transportation between laboratories, can all lead to RNA degradation. Therefore, it would seem that, before employing RNA samples in downstream applications, a thorough evaluation of RNA integrity is necessary (Vermeulen et al., 2011). Table 8 provides the RINs of patient samples in the good and poor responder categories. An RIN of 1,4 (with 1 indicating totally degraded to 10 for completely intact RNA) has been successfully employed in gene expression assays (Kokkat et al., 2013). In the good responder category, the average RIN ranged from a minimum of 2.1 to a maximum of 3.0, with an average of 2.41. The RIN of patients in the poor responder category, ranged

from a minimum of 1.7 to a maximum of 3.8, with an average of 2.61. These results are consistent with those from a similar study published by Choi et al (2017) who reported RINs which ranged from 1.0 to 6.9, with averages of 1.25 to 3.43, although their focus was on the FFPE samples of breast cancer.

A SPUD assay, which is a quantitative PCR-based assay was employed to assess the purity of the RNA samples by detecting PCR (enzyme) inhibitors (Vermeulen et al., 2011). Table 9 presented the Cq values within the 0.09 cycle of the negative control for both categories. They indicated that the patient samples were free of inhibitors. According to (Vermeulen et al., 2011), a Cq>1 is used as a cut-off point to indicate the presence of SPUD assay inhibitors.

The 5'-3' integrity assay was used to assess the integrity of a reference gene mRNA, which is thought to be an accurate indicator of the integrity of all the mRNAs in a particular RNA sample. This qPCR-based assay's fundamental premise is that anchored oligo-dT primed reverse transcription starts at the 3' poly-A tail and ends at the 5' start, stopping if mRNA fragmentation results from degradation (Vermeulen et al., 2011). Two different primer sets are used - one annealing near the 5′-end and the other pair targeting a sequence near the 3′-end of a reference gene (e.g., GAPDH). Oligo(dT)-primed cDNA is generated from an RNA sample and used as a template for qPCR with each 5' and 3' primer set. Cq values are then determined for each assay, and the difference in Cq values between the two assays (∆Cq5'-3') is calculated and compared to that derived from a sample using high quality RNA. The more degraded the RNA sample, the higher the Cq difference between the two assays and that of the control sample. Table 10 displays the results of the 5'-3' integrity assay. The 5' Cq's were below the level of detection for half of the patient samples in both the good and poor responder categories. Therefore, the ∆Cq5'-3' could not be calculated.

The results for the qPCR validation and specificity assay are represented in Figure 10.1 (A-F) in the form of standard curves, PCR efficiencies and melt curves of ABCC1/MRP1, ABCC2/MRP2, and ABCC10/MRP7 transporter genes.

The PCR efficiencies of ABCC1, ABCC2, and ABCC10 were 103,962%, 105, 542% and 117,96% respectively. The ideal efficiency is 100%, but an efficiency in the range of 90-

110% is acceptable according to the MIQE guidelines (Bustin et al., 2009). The qPCR primers used in this study showed qPCR efficiencies within the acceptable range and with high linearity ($R^2 \geq 0.99$) except for ABCC10 (E= 117,96%).

Furthermore, the melting curves of ABCC1, ABCC2, and ABCC10 show that there was no variation between the amplicon (PCR product). This indicates that there was no non-specific binding, but that the binding was specific to the primers, hence the uniformity that is observed in the melting curves. All qPCR assays showed single amplicons as shown by single Tm peaks on the melt curves, indicating that there was no primer dimer formation.

The above-mentioned quality control assays employed on the RNA samples of patients in the good and poor responder categories were essential to ensure that the samples were of sufficient quantity and good quality to be utilized in quantitative RT-PCR for the evaluation of the expression levels of ABC-transporter genes (ABCC1/MRP1, ABCC2/MRP2, and ABCC10/MRP7). Table 15 provides the relative expression levels of ABCC1, ABCC2, and ABCC10 drug transporters in the poor and good responder categories, obtained through quantitative RT-PCR. All three ABC-transporter genes were expressed in the FFPE tissue biopsies of PCa patients, in varying amounts.

In the good responders' category, the average expression levels of ABCC1, ABCC2, and ABCC10 were 20-50-fold higher in the normal sections, than in the tumour sections of the patient samples. ABCC2's average expression levels were higher in both the (T) and (N) sections of patients in the good responder category in comparison to ABCC1 and ABCC10. For the poor responders' category, the average expression levels of ABCC1 and ABCC10 were 3-5-fold higher in the tumour sections, than in the normal sections of the patient samples. ABCC10 had the highest average expression levels in the (T) and (N) sections of patients in the poor responder category compared to ABCC1.

When comparing the average relative expression levels in the (T) sections of patients in the good responder category, with the average expression levels in the (T) sections of patients in the poor responders category, it was observed that the average expression levels of ABCC1 and ABCC10 in the (T) sections of patients in the poor responder

category were higher than the average expression levels of ABCC1 and ABCC10 in the (T) sections of patients in the good responder category.

The opposite was observed for the average expression levels of ABCC1/MRP1, ABCC2/MRP2, and ABCC10/MRP7 in the (N) sections of patients in the good and poor responder categories. ABCC1/MRP1, ABCC2/MRP2, and ABCC10/MRP7's average expression levels in the (N) sections of patients in the good responder category, were much higher than in the (N) sections of patients in the poor responder category. Based on the research findings, we could infer that the patients in the good responder category had good treatment responses because the average expression levels of ABC-transporter genes (ABCC1/MRP1 and ABCC10/MRP7) in the (T) sections of these patients were lower, when compared to the average expression levels of the same transporter genes in the (T) sections of patients in the poor responder category, which were higher. Therefore, the drug could have had sufficient time to have an effect on the tumour, and for the drug's concentration to increase in the system of the PCa patient, which in turn could have led to an improvement in the patients' condition.

Moreover, the inference could be made that patients in the poor responder category possibly had poor treatment outcomes because the average expression levels of the ABC-transporter genes (ABCC1/MRP1 and ABCC10/MRP7) in their (T) sections were higher. Therefore, the chemotherapeutic agent (docetaxel) could not have sufficient time to sensitize and produce its therapeutic effect on the PCa tumour, before being effluxed by the ABCC1/MRP1 and ABCC10/MRP7 transporters. So, this in turn, could have caused the intracellular concentrations of the drug in the PCa patients to remain low, which in the long run could have contributed to acquired drug resistance in the patients, which resulted in no improvement in the condition of the patient. The results from this study are consistent with a study published by (Karatas et al., 2016), who reported an increase in the expression levels of ABCC1 and ABCC2 in the tumour samples compared to normal samples. The difference in the findings observed in the research of (Karatas et al., 2016) and this study, is that their research used tissues obtained from radical prostatectomies (surgery) of PCa patients for extraction of RNA, whereas this study utilised FFPE tissue blocks of PCa patients. In addition, their study reported that the

expression levels of ABCC10 remained unchanged in the tumour and normal prostate tissues, whereas this study discovered that the ABCC10's average expression levels were increased in the tumour sections of the PCa patients in the poor responder category but were lower in its normal sections.

Overexpression of ABC-transporters can enhance drug efflux and lower cytoplasmic drug concentration, which leads to decreased efficacy and possibly a drug-resistant phenotype (Sone et al., 2019). Although the results of ABCC2 in the poor responders' category was not an adequate representation of its expression levels because it could not be determined in half the patients' samples, ABCC2 plays a vital role in the metabolism of docetaxel. Also, it has been documented that single nucleotide polymorphisms in this transporter gene impacts the clinical outcome of patients treated with docetaxel. Moreover, ABCC10/MRP7 has been reported to confer resistance to docetaxel and other taxanes (Sone et al., 2019). Lastly, increased expression levels of ABCC1/MRP1 have been observed in PCa clinically, and it has been associated with clinical outcomes (Chen and Tiwari, 2011, Sodani et al., 2012) . Therefore, the above-mentioned literature on these ABC-transporter genes provides a possible explanation for the expression levels of ABCC1/MRP1, ABCC2/MRP2, and ABCC10/MRP7 observed in the FFPE tissues of PCa patients. The patient population in this study, was treated with 2-10 cycles in months, of docetaxel. The good responder category was sensitive to docetaxel and showed improvement, while the poor responder category was resistant to docetaxel and showed no improvement. The varied expression levels of the transporter genes in each of the tissue sections of the patients, provides a possible explanation for the different treatment outcomes observed in each patient category.

The upregulation of ABCC1 and ABCC10 in the tumour sections of PCa patients in the poor responder's category has notable importance for clinical practice. Firstly, an understanding of these ABC-transporter genes could potentially assist clinicians to tailor their treatment regimens. Individualized methods may include considering alternate chemotherapeutic agents or changing dosages to combat resistance.

Secondly, the expression levels of ABCC1 and ABCC10 can be used as predictive biomarkers to measure possible docetaxel resistance. This knowledge could assist

clinicians in making timely modifications to treatment regimens. Also, the findings of the upregulation of these ABC-transporter genes in the tumour sections of PCa patients in the poor responder's category, highlight the importance of combining docetaxel with drugs that can inhibit these ABC-transporter genes. This combination approach may assist in combating resistance and potentially improve therapeutic efficacy.

Proteins were also extracted from the FFPE tissue blocks of patients in the good and poor responder categories, using the protein extraction without acetone purification method. These proteins were then quantified using the BCA assay for later use in the western blot assay. The BCA (bicinchoninic acid) protein assay is a detergent-compatible formulation for colourimetric detection and quantification of total protein that is based on the BCA. This technique combines the highly sensitive and selective colourimetric detection of the cuprous ion (Cu^{+1}) using a special reagent containing BCA, with the well-known reduction of Cu^{+2} to Cu^{+1} by protein in an alkaline solution. Two molecules of BCA chelate with one Cu^{+1} to create the assay's purple-coloured reaction result over a wide working range (25 – 2000 µg/ml). This water-soluble compound shows high absorbance at 562 nm which is nearly linear with increasing protein concentrations. As a result, protein concentrations are typically calculated and reported using common protein standards, including bovine serum albumin (BSA). Table 16 shows the protein concentrations of proteins extracted without acetone purification method. The protein concentrations of the patients in the good and poor responder categories were all above 200 µg/ml, except for sample 5N in the good responders' category. The protein concentration results are consistent with a similar study published by (Kokkat et al., 2013) which reported concentrations above 200 µg/ml from proteins extracted from FFPE tissues, although they extracted proteins from the FFPE tissue blocks of patients with different cancers (malignant lung, thyroid, and salivary gland).

Following protein quantification, protein expression analysis assay was employed to determine the expression of MRP1, MRP2 and MRP7 in the protein samples of patients in the good and poor responder categories. The results from the assay were not recorded in the results section, as it was unsuccessful. MRP1 was not expressed in any of the patient samples in either category. These results are consistent with a similar study

published by (Sánchez et al., 2009), who reported that MRP1 protein was not expressed in the PCa cell lines (LNCap, PC3 and DU145) using a western blot assay. To determine whether the reason for MRP1 not being expressed in any of the patient samples was due to a low MRP1 antibody concentration, or due to the protein concentrations of the patient samples not being high enough, an additional step was incorporated. HepG2 cells were cultured, and the proteins extracted and quantified using the BCA assay (see Table 17). Following quantification, the protein concentration of the HepG2 cells was diluted (500 µg/ml – 15,625 µg/ml). The purpose of incorporating this step was to determine the lowest protein concentration which could be loaded on an SDS-page, while still enabling observation of protein bands in a western blot assay. This cell line was selected because it was the available cell line at the time (convenience sampling). Due to the reasoning behind this step, it was not necessary to specifically use a PCa cell line.

Following calculation of half dilutions of the HepG2 protein concentration, western blot assay was carried out. However, the transfer of proteins onto a membrane and subsequent probing of anti-MRP1 and housekeeping protein Beta-actin, yielded no results. Following this, a further investigation was conducted, using an imperial protein stain assay to determine whether there was any protein present in the protein samples of the patients, as well as in the HepG2 protein samples, as confirmed by the BCA assay. The imperial stain is a dye-based reagent for Coomassie R-250 that is used to stain proteins on polyacrylamide gels. This sensitive (≤3ng) stain produces an intense colour that photographs well. Only proteins are stained by this reagent, which also makes it possible to see bands in the gels right away after staining. Figures 15 and 16 show the imperial stain gels of patients in the good and poor responder categories. No protein bands were detected in any of the categories using this stain. To confirm whether the protein staining assay was accurate, another staining assay was performed using HepG2 protein concentrations. Figure 17 clearly shows the detection of proteins in the form of bands. As the protein concentration became lower, it was observed that the expression of the bands became lighter. `The success of this assay, using HepG2 cells, indicated that the problem (non-visibility of bands on the gel) could possibly lie in the proteins extracted from the FFPE tissues. The results of the HepG2 cells protein stain are consistent with a similar study published by (Gauci et al., 2011), who reported visible

protein bands from the Coomassie brilliant blue stain on HepG2 and HepG2.2.15 cells. Due to time constraints and expended consumables, the remaining analysis for protein expression of MRP2 and MRP7, could not be carried out.

CHAPTER 6:

CONCLUSION

The present study focused on investigating the expression levels of ABC-transporter genes (ABCC1/MRP1, ABCC2/MRP2, and ABCC10/MRP7) as potential, predictive biomarkers in PCa patients, which could be employed in the future as a diagnostic tool, to determine docetaxel treatment outcome in PCa patients, before they undergo treatment.

6.1 The extent to which the study objectives were achieved

RNA was successfully extracted from the FFPE tissues of patients in the good and poor responder categories. FFPE tissues seem to be a reliable mechanism of long storage of samples and results obtained from their use are comparable to results obtained from using fresh samples (Karatas et al., 2016). Successive quality control assays were employed on the RNA samples to ensure that they were of sufficient quantity and quality to be utilized in quantitative RT-PCR for the determination of the expression levels of ABCC1/MRP1, ABCC2/MRP2, and ABCC10/MRP7. As stated in the results section, all three transporter genes were expressed in the PCa samples of patients in the good and poor responder categories. ABCC2 displayed the highest average expression levels in both the (T) and (N) sections of patients in the good responder category, in comparison to ABCC1 and ABCC10. ABBC10 showed elevated expression levels in the (T) and (N) sections of patients in the poor responder category when compared to ABCC1 and ABCC2. Overall, it was observed that the average relative expression levels of ABCC1 and ABCC10 in the (T) sections of patients in the poor responder category were higher than in the (T) sections of patients in the good responder category.

Furthermore, the average relative expression levels of ABCC1, ABCC2 and ABCC10 in the (N) sections of patients in the good responder category were higher than in the (N) sections of patients in the poor responder category. For this reason, it can be deduced that the good treatment outcomes observed in patients in the good responder category,

could possibly be due to the low expression levels of ABCC1/MRP1, ABCC2/MRP2 and ABCC10/MRP7 in their (T) sections. Also, the reason for the PCa patients in the poor responder category showing poor treatment outcomes, could be due to the elevated expression levels of ABCC1 and ABBC10 observed in the (T) sections of the patient samples, in comparison with the good responder category. Therefore, it could be concluded that a correlation exists between ABCC1 and ABCC10 expression levels and drug resistance experienced by patients in the poor responder category. Also, the detection of transporter genes ABCC1, ABCC2 and ABCC10 could potentially be used as indicators for possible treatment outcomes. Unfortunately, a proper analysis of ABCC2's average relative expression levels in the poor responder category could not be carried out because the expression levels for half of the patients in this category could not be determined. Thus, a thorough comparison could not be drawn between the expression levels of ABCC2 in the (T) and (N) sections of patients in the good and poor responder categories, as was achieved with ABCC1 and ABCC10. Lastly, MRP1/ABCC1, MRP2/ABCC2, and MRP7/ABCC10 play a role in MDR, and their varied expression levels in the FFPE tissue sections of PCa patients, could have contributed to the good or poor treatment outcomes experienced by the PCa patients in this study, treated with docetaxel.

Finally, proteins were also successfully extracted from the FFPE tissues of PCa patients and quantified. However, the expression of MRP1 was unsuccessful in the western blot assay and proteins could not be detected with the Coomassie R-250 staining assay. As a result, the expression of MRP2 and MRP7 was not further investigated using a western blot assay due to time constraints and expended consumables. Ultimately, there was no correlation between the expression of these transporter proteins (MRP1, MRP2 and MRP7), and good or poor treatment responses in PCa patients, using western blot analysis.

Future suggestions include that RNA and protein extraction kits, which are well known and reported in most studies such as the AllPrep DNA/RNA FFPE kit (Qiagen) and Qproteome FFPE tissue kit (Qiagen), be employed in the extraction of RNA and proteins to try and mitigate low RNA concentrations and the lack of protein detection in western blot assays (Guo et al., 2012, Kokkat et al., 2013, Yi et al., 2020). Furthermore, additional

assays can be incorporated for protein visualization and detection in samples, such as liquid chromatography mass spectrometry (LC-MS).

6.2 Limitations of the study

The limitation of the study is that there are other mechanisms that contribute to chemo resistance, such as suppression of cell programmed death; decreased uptake of water-soluble drugs and upregulation of some heat shock proteins in PCa tissue, in comparison to normal prostate tissue (Mahon et al., 2011, Kachalaki et al., 2016). Furthermore, it has been reported that cytochrome P450 (CYP) subfamily 3A and 2C enzymes significantly contribute to the metabolism of taxanes (docetaxel & paclitaxel) (van Eijk et al., 2019). This, in turn, can result in the poor treatment outcomes observed in patients. The correlation of *in vitro* results with observed clinical outcomes is affected by factors such as metabolism, absorption, stability, and solubility of the drug. Therefore, it is vital to note that the findings from this study are not comprehensive and the only direct influence of the treatment outcomes because it is an *in vitro* study. The findings provided an explanation at a proteomic and genetic level.

Based on the research findings, the above-mentioned mechanisms which also contribute to resistance, did not affect the results of the study. This is because the focus of the study was on the mechanism of increased drug efflux caused by ABC-transporter genes. Therefore, the methodologies employed in this study were specifically targeting ABC-transporter genes (ABCC1, ABCC2, and ABCC10). To address this limitation in the future, would require research studies to be undertaken with methodologies that target the above-mentioned mechanisms which contribute to chemoresistance in PCa.

The additional limitation is that the good responder category only had four patient samples instead of five, with both the tumour and normal sections from the provided FFPE tissue blocks, which could be excised. This was due to the fifth patients' FFPE tissue block having 100% tumour tissue, and no normal tissue, which could be used as the control. This limitation did not negatively impact the results of the study, because the findings highlighted that the ABC-transporter genes were upregulated in the tumour sections of

the PCa patients in the poor responder's category, and not the good responder's category.

With regards to the expression levels of ABC-transporter genes (ABCC1, ABCC2, and ABCC10), the average expression levels of ABCC2/MRP2 in the (T) and (N) sections of patients in the poor responder category could not be compared to the (T) and (N) sections of patients in the good responder category, because the expression levels for half of the patient samples in the poor responder's category could not be determined.

6.3 Possible future studies

Due to the rising prevalence of PCa, South Africa, stands to gain from novel diagnostics developed under pharmacogenomics research. The potential for employing genome-based technology to treat diseases more effectively through pharmacogenomic applications is promising.

The majority of research on significant pharmacogenes in South African populations to date, has focused on genes encoding members of the major drug-metabolizing family, known as the cytochrome P450 enzymes (CYP enzymes). These enzymes are crucial for phase 1 metabolism of both endogenous and exogenous compounds, including medicines utilized in HIV/AIDS treatment (Warnich et al., 2011).

Therefore, there is a need to carry out more research in the search for biomarkers or pharmacogenes which contribute to poor treatment outcome or resistance in South African PCa patients. Future studies could focus on investigating the expression of Heat Shock proteins (HSP) such as HSP27 and HSP90 as potential biomarkers, in PCa patients, as a mechanism which can potentially contribute to tumour resistance, bone metastasis and invasion which results in PCa being more difficult to treat (Hoter et al., 2018, Lampros et al., 2022). A larger sample size of PCa patients can be employed in future retrospective studies. Pharmacogenomics has the potential to enhance a nation's capacity to address disease threats such as PCa.

References

Chemotherapy for Prostate Cancer [Online]. American Cancer Society. Available: https://www.cancer.org/cancer/types/prostate-cancer/treating/chemotherapy.html [Accessed 23 July 2021].

Estimated number of deaths in 2020, prostate, males, ages 40-84 [Online]. France: Globocan. Available: https://gco.iarc.fr/today/online-analysis-table?v=2020&mode=population&mode_population=regions&population=900&populations=900&key=asr&sex=1&cancer=27&type=1&statistic=5&prevalence=0&population_group=0&ages_group%5B%5D=8&ages_group%5B%5D=16&group_cancer=0&include_nmsc=0&include_nmsc_other=1 [Accessed 03 October 2023].

Hormone Therapy for Prostate Cancer [Online]. American Cancer Society. Available: https://www.cancer.org/cancer/types/prostate-cancer/treating/hormone-therapy.html [Accessed 23 July 2021].

How Biopsy and Cytology Samples are Processed [Online]. American Cancer Society. Available: https://www.cancer.org/cancer/diagnosis-staging/tests/biopsy-and-cytology-tests/testing-biopsy-and-cytology-samples-for-cancer/how-samples-are-processed.html [Accessed 25 September 2023].

Immunotherapy for Prostate Cancer [Online]. American Cancer Society. Available: https://www.cancer.org/cancer/types/prostate-cancer/treating/vaccine-treatment.html [Accessed 17 August 2021].

Medical Illustrations [Online]. emedicinehealth. Available: https://www.emedicinehealth.com/image-gallery/prostate_picture/images.htm [Accessed 03 October 2023].

Observation or Active Surveillance for Prostate Cancer [Online]. American Cancer Society. Available: https://www.cancer.org/cancer/types/prostate-cancer/treating/watchful-waiting.html [Accessed 26 November 2023].

Prostate Cancer Stages [Online]. American Cancer Society. Available: https://www.cancer.org/cancer/types/prostate-cancer/detection-diagnosis-staging/staging.html [Accessed 31 May 2021].

Prostate Cancer Treatment (PDQ) - Patient version [Online]. National Cancer Institute. Available: https://www.cancer.gov/types/prostate/patient/prostate-treatment-pdq#_102 [Accessed 17 August 2021].

Prostate Cancer: Types of Treatment [Online]. Cancer.net. Available: https://www.cancer.net/cancer-types/prostate-cancer/types-treatment [Accessed 26 November 2023].

The Prostate Gland [Online]. TeachMe Anatomy. Available: https://teachmeanatomy.info/pelvis/the-male-reproductive-system/prostate-gland/ [Accessed 01 April 2022].

Prostate gland [Online]. Mayo Clinic. Available: https://www.mayoclinic.org/diseases-conditions/prostate-cancer/multimedia/prostate-gland/img-20006060 [Accessed 06 November 2023].

What is Prostate Cancer? [Online]. American Cancer Society. Available: https://www.cancer.org/cancer/types/prostate-cancer/about/what-is-prostate-cancer.html [Accessed 31 May 2021].

ABIDI, A. 2013. Cabazitaxel: A novel taxane for metastatic castration-resistant prostate cancer-current implications and future prospects. *Journal of Pharmacology and Pharmacotherapeutics,* 4**,** 230-237.

AUTA, T. & HASSAN, A. 2016. Reproductive toxicity of aqueous wood-ash extract of Azadirachta indica (neem) on male albino mice. *Asian Pacific Journal of Reproduction,* 5**,** 111-115.

BABB, C., URBAN, M., KIELKOWSKI, D. & KELLETT, P. 2014. Prostate cancer in South Africa: pathology based national cancer registry data (1986–2006) and mortality rates (1997–2009). *Prostate cancer,* 2014.

BEGICEVIC, R.-R. & FALASCA, M. 2017. ABC transporters in cancer stem cells: beyond chemoresistance. *International journal of molecular sciences,* 18**,** 2362.

BERGENGREN, O., PEKALA, K. R., MATSOUKAS, K., FAINBERG, J., MUNGOVAN, S. F., BRATT, O., BRAY, F., BRAWLEY, O., LUCKENBAUGH, A. N. & MUCCI, L. 2023. 2022 Update on Prostate Cancer Epidemiology and Risk Factors—A Systematic Review. *European Urology*.

BERNSTEIN, C., PRASAD, A. R., NFONSAM, V. & BERNSTEIN, H. 2013. *DNA damage, DNA repair and cancer*, InTech Rijeka, Croatia.

BUSTIN, S. A., BENES, V., GARSON, J. A., HELLEMANS, J., HUGGETT, J., KUBISTA, M., MUELLER, R., NOLAN, T., PFAFFL, M. W. & SHIPLEY, G. L. 2009. The MIQE Guidelines: M inimum I nformation for Publication of Q uantitative Real-Time PCR E xperiments. Oxford University Press.

BUSZEWSKA-FORAJTA, M., PATEJKO, M., MACIOSZEK, S., SIGORSKI, D., IŻYCKA-ŚWIESZEWSKA, E. & MARKUSZEWSKI, M. J. 2019. Paraffin-embedded tissue as a novel matrix in metabolomics study: optimization of metabolite extraction method. *Chromatographia,* 82**,** 1501-1513.

CALABRÒ, F. & STERNBERG, C. N. 2007. Current indications for chemotherapy in prostate cancer patients. *European urology,* 51**,** 17-26.

CASSIM, N., AHMAD, A., WADEE, R., REBBECK, T., GLENCROSS, D. & GEORGE, J. 2021. Prostate cancer age-standardised incidence increase between 2006 and 2016 in Gauteng Province, South Africa: A laboratory data-based analysis. *South African Medical Journal,* 111**,** 26-32.

CHEN, X.-Y., YANG, Y., WANG, J.-Q., WU, Z.-X., LI, J. & CHEN, Z.-S. 2021. Overexpression of ABCC1 confers drug resistance to betulin. *Frontiers in oncology,* 11**,** 640656.

CHEN, Z. S. & TIWARI, A. K. 2011. Multidrug resistance proteins (MRPs/ABCCs) in cancer chemotherapy and genetic diseases. *The FEBS journal,* 278**,** 3226-3245.

CHENG, L., MONTIRONI, R., BOSTWICK, D. G., LOPEZ-BELTRAN, A. & BERNEY, D. M. 2012. Staging of prostate cancer. *Histopathology,* 60**,** 87-117.

CHOI, C.-H. 2005. ABC transporters as multidrug resistance mechanisms and the development of chemosensitizers for their reversal. *Cancer cell international,* 5**,** 1-13.

CHOI, Y., KIM, A., KIM, J., LEE, J., LEE, S. Y. & KIM, C. 2017. Optimization of RNA extraction from formalin-fixed paraffin-embedded blocks for targeted next-generation sequencing. *Journal of Breast Cancer,* 20**,** 393-399.

DAS, C. J., NETAJI, A., RAZIK, A. & VERMA, S. 2020. MRI-targeted prostate biopsy: what radiologists should know. *Korean journal of radiology,* 21**,** 1087.

DOMENICHINI, A., ADAMSKA, A. & FALASCA, M. 2019. ABC transporters as cancer drivers: Potential functions in cancer development. *Biochimica et Biophysica Acta (BBA)-General Subjects,* 1863**,** 52-60.

DRAISMA, G., POSTMA, R., SCHRÖDER, F. H., VAN DER KWAST, T. H. & DE KONING, H. J. 2006. Gleason score, age and screening: modeling dedifferentiation in prostate cancer. *International journal of cancer,* 119**,** 2366-2371.

GAUCI, V. J., WRIGHT, E. P. & COORSSEN, J. R. 2011. Quantitative proteomics: assessing the spectrum of in-gel protein detection methods. *Journal of chemical biology,* 4**,** 3-29.

GILLIGAN, T. & KANTOFF, P. W. 2002. Chemotherapy for prostate cancer. *Urology,* 60**,** 94-100.

GOMELLA, L. G., JOHANNES, J. & TRABULSI, E. J. 2009. Current prostate cancer treatments: effect on quality of life. *Urology,* 73**,** S28-S35.

GRAY, P. B., MEINTJES, F., MOSHOKOA, E. & MATHABE, K. 2020. A qualitative exploration of South African men's perceived effects of Androgen Deprivation Therapy (ADT) as a treatment for advanced prostate cancer. *The Aging Male,* 23**,** 1266-1274.

GRÖNBERG, H. 2003. Prostate cancer epidemiology. *The Lancet,* 361**,** 859-864.

GUO, H., LIU, W., JU, Z., TAMBOLI, P., JONASCH, E., MILLS, G. B., LU, Y., HENNESSY, B. T. & TSAVACHIDOU, D. 2012. An efficient procedure for protein extraction from formalin-fixed, paraffin-embedded tissues for reverse phase protein arrays. *Proteome science,* 10**,** 1-12.

HAHN, A. W., HIGANO, C. S., TAPLIN, M.-E., RYAN, C. J. & AGARWAL, N. 2018. Metastatic castration-sensitive prostate cancer: optimizing patient selection and treatment. *American Society of Clinical Oncology Educational Book,* 38**,** 363-371.

HASAN, S., TAHA, R. & EL OMRI, H. 2018. Current opinions on chemoresistance: An overview. *Bioinformation,* 14**,** 80.

HOPPER-BORGE, E., XU, X., SHEN, T., SHI, Z., CHEN, Z.-S. & KRUH, G. D. 2009. Human multidrug resistance protein 7 (ABCC10) is a resistance factor for nucleoside analogues and epothilone B. *Cancer research,* 69**,** 178-184.

HOTER, A., EL-SABBAN, M. E. & NAIM, H. Y. 2018. The HSP90 family: structure, regulation, function, and implications in health and disease. *International journal of molecular sciences,* 19**,** 2560.

IKEDA, K., MONDEN, T., KANOH, T., TSUJIE, M., IZAWA, H., HABA, A., OHNISHI, T., SEKIMOTO, M., TOMITA, N. & SHIOZAKI, H. 1998. Extraction and analysis of diagnostically useful proteins from formalin-fixed, paraffin-embedded tissue sections. *Journal of Histochemistry & Cytochemistry,* 46**,** 397-403.

ITTMANN, M. 2018. Anatomy and histology of the human and murine prostate. *Cold Spring Harbor perspectives in medicine,* 8.

KACHALAKI, S., EBRAHIMI, M., KHOSROSHAHI, L. M., MOHAMMADINEJAD, S. & BARADARAN, B. 2016. Cancer chemoresistance; biochemical and molecular aspects: a brief overview. *European journal of pharmaceutical sciences,* 89**,** 20-30.

KARATAS, O. F., GUZEL, E., DUZ, M. B., ITTMANN, M. & OZEN, M. 2016. The role of ATP-binding cassette transporter genes in the progression of prostate cancer. *The Prostate,* 76**,** 434-444.

KEYES, M., CROOK, J., MORTON, G., VIGNEAULT, E., USMANI, N. & MORRIS, W. J. 2013. Treatment options for localized prostate cancer. *Canadian Family Physician,* 59**,** 1269-1274.

KOBEISSY, F., SHAITO, A., KAPLAN, A., BAKI, L., HAYEK, H., DAGHER-HAMALIAN, C., NEHME, A., GHALI, R., ABIDI, E. & HUSARI, A. 2017. Acute exposure to cigarette smoking followed by myocardial infarction aggravates renal damage in an in vivo mouse model. *Oxidative medicine and cellular longevity,* 2017.

KOKKAT, T. J., PATEL, M. S., MCGARVEY, D., LIVOLSI, V. A. & BALOCH, Z. W. 2013. Archived formalin-fixed paraffin-embedded (FFPE) blocks: a valuable underexploited resource for extraction of DNA, RNA, and protein. *Biopreservation and biobanking,* 11**,** 101-106.

LAMPROS, M., VLACHOS, N., VOULGARIS, S. & ALEXIOU, G. A. 2022. The role of hsp27 in chemotherapy resistance. *Biomedicines,* 10**,** 897.

LIMA, T. S., IGLESIAS-GATO, D., SOUZA, L. D., STENVANG, J., LIMA, D. S., RØDER, M. A., BRASSO, K. & MOREIRA, J. M. 2021. Molecular profiling of docetaxel-resistant prostate cancer cells identifies multiple mechanisms of therapeutic resistance. *Cancers,* 13**,** 1290.

MAHON, K. L., HENSHALL, S. M., SUTHERLAND, R. L. & HORVATH, L. G. 2011. Pathways of chemotherapy resistance in castration-resistant prostate cancer. *Endocrine-related cancer,* 18**,** R103-R123.

MUAZZAM, A., SPICK, M., CEXUS, O. N., GEARY, B., AZHAR, F., PANDHA, H., MICHAEL, A., REED, R., LENNON, S. & GETHINGS, L. A. 2023. A novel blood proteomic signature for prostate cancer. *Cancers,* 15**,** 1051.

NADER, R., EL AMM, J. & ARAGON-CHING, J. B. 2018. Role of chemotherapy in prostate cancer. *Asian journal of andrology,* 20**,** 221.

NAJI, L., RANDHAWA, H., SOHANI, Z., DENNIS, B., LAUTENBACH, D., KAVANAGH, O., BAWOR, M., BANFIELD, L. & PROFETTO, J. 2018. Digital rectal examination for prostate cancer screening in primary care: a systematic review and meta-analysis. *The Annals of Family Medicine,* 16**,** 149-154.

NARAYAN, V., ROSS, A., PARIKH, R., NOHRIA, A. & MORGANS, A. 2021. How to Treat Prostate Cancer With Androgen Deprivation and Minimize Cardiovascular Risk: A Therapeutic Tightrope. *JACC CardioOncology,* 3**,** 737-741.
NOLAN, T., HANDS, R. E. & BUSTIN, S. A. 2006. Quantification of mRNA using real-time RT-PCR. *Nature protocols,* 1**,** 1559-1582.

Parker, C., Gillessen, S., Heidenreich, A. and Horwich, A., 2015. Cancer of the prostate: ESMO Clinical Practice Guidelines for diagnosis, treatment and follow-up. *Annals of Oncology*, *26*, pp.v69-v77.

PARRA-MEDINA, R. & RAMÍREZ-CLAVIJO, S. 2021. Why not to use punch biopsies in formalin-fixed paraffin-embedded samples of prostate cancer tissue for DNA and RNA extraction? *African Journal of Urology,* 27**,** 154.

QUINN, D., SANDLER, H., HORVATH, L., GOLDKORN, A. & EASTHAM, J. 2017. The evolution of chemotherapy for the treatment of prostate cancer. *Annals of Oncology,* 28**,** 2658-2669.

RAWLA, P. 2019. Epidemiology of prostate cancer. *World journal of oncology,* 10**,** 63.
RODRIGUES-FERREIRA, S., MOINDJIE, H., HAYKAL, M. M. & NAHMIAS, C. 2021. Predicting and overcoming taxane chemoresistance. *Trends in Molecular Medicine,* 27**,** 138-151.

SÁNCHEZ, C., MENDOZA, P., CONTRERAS, H. R., VERGARA, J., MCCUBREY, J. A., HUIDOBRO, C. & CASTELLON, E. A. 2009. Expression of multidrug resistance proteins in prostate cancer is related with cell sensitivity to chemotherapeutic drugs. *The Prostate,* 69**,** 1448-1459.

SARHADI, V. K. & ARMENGOL, G. 2022. Molecular biomarkers in cancer. *Biomolecules,* 12**,** 1021.

SAVARD, J., HERVOUET, S. & IVERS, H. 2013. Prostate cancer treatments and their side effects are associated with increased insomnia. *Psycho-Oncology,* 22**,** 1381-1388.

SHAH, R. B. & ZHOU, M. 2019. Anatomy and Normal Histology of the Prostate Pertinent to Biopsy Interpretation. *Prostate Biopsy Interpretation.* Second edition ed. Switzerland: Springer Nature Switzerland AG, pp 1-2.

SHAROM, F. J. 2008. ABC multidrug transporters: structure, function and role in chemoresistance.

SHELLEY, M., WILT, T. J., COLES, B. & MASON, M. 2007. Cryotherapy for localised prostate cancer. *Cochrane Database of Systematic Reviews*.

SHI, S.-R., LIU, C., BALGLEY, B. M., LEE, C. & TAYLOR, C. R. 2006. Protein extraction from formalin-fixed, paraffin-embedded tissue sections: quality evaluation by mass spectrometry. *Journal of Histochemistry & Cytochemistry,* 54**,** 739-743.

SODANI, K., PATEL, A., KATHAWALA, R. J. & CHEN, Z.-S. 2012. Multidrug resistance associated proteins in multidrug resistance. *Chinese journal of cancer,* 31**,** 58.

SONE, K., OGURI, T., UEMURA, T., TAKEUCHI, A., FUKUDA, S., TAKAKUWA, O., MAENO, K., FUKUMITSU, K., KANEMITSU, Y. & OHKUBO, H. 2019. Genetic variation in the ATP binding cassette transporter ABCC10 is associated with neutropenia for docetaxel in Japanese lung cancer patients cohort. *BMC cancer,* 19**,** 1-9.

SOORIAKUMARAN, P., SIEVERT, K.-D., SRIVASTAVA, A. & TEWARI, A. 2012. Applied Anatomy of the Prostate. *In:* DASGUPTA, P. & KIRBY, R. S. (eds.) *ABC of Prostate Cancer.* 1st ed. UK: Blackwell Publishing Ltd. pp 1.

SUN, B., STRAUBINGER, R. M. & LOVELL, J. F. 2018. Current taxane formulations and emerging cabazitaxel delivery systems. *Nano Research,* 11**,** 5193-5218.

SUNG, H., FERLAY, J., SIEGEL, R. L., LAVERSANNE, M., SOERJOMATARAM, I., JEMAL, A. & BRAY, F. 2021. Global cancer statistics 2020: GLOBOCAN estimates of incidence and mortality worldwide for 36 cancers in 185 countries. *CA: a cancer journal for clinicians,* 71**,** 209-249.

TEPLY, B. A., LUBER, B., DENMEADE, S. R. & ANTONARAKIS, E. S. 2016. The influence of prednisone on the efficacy of docetaxel in men with metastatic castration-resistant prostate cancer. *Prostate cancer and prostatic diseases,* 19**,** 72-78.

TOPS, S. C., GROOTENHUIS, J. G., DERKSEN, A. M., GIARDINA, F., KOLWIJCK, E., WERTHEIM, H. F., SOMFORD, D. M. & SEDELAAR, J. M. 2022. The effect of different types of prostate biopsy techniques on post-biopsy infectious complications. *The Journal of Urology,* 208**,** 109-118.

VAN EIJK, M., BOOSMAN, R. J., SCHINKEL, A. H., HUITEMA, A. D. & BEIJNEN, J. H. 2019. Cytochrome P450 3A4, 3A5, and 2C8 expression in breast, prostate, lung, endometrial, and ovarian tumors: relevance for resistance to taxanes. *Cancer chemotherapy and pharmacology,* 84**,** 487-499.

VARMA, M. & CHANDRA, A. 2012. Pathology of Prostate Cancer. *In:* DASGUPTA, P. & KIRBY, R. S. (eds.) *ABC of Prostate Cancer.* 1st ed. UK: Blackwell Publishing Ltd, pp 5-7.

VARNAI, R., KOSKINEN, L. M., MÄNTYLÄ, L. E., SZABO, I., FITZGERALD, L. M. & SIPEKY, C. 2019. Pharmacogenomic biomarkers in docetaxel treatment of prostate cancer: from discovery to implementation. *Genes,* 10**,** 599.

VERMEULEN, J., DE PRETER, K., LEFEVER, S., NUYTENS, J., DE VLOED, F., DERVEAUX, S., HELLEMANS, J., SPELEMAN, F. & VANDESOMPELE, J. 2011.

Measurable impact of RNA quality on gene expression results from quantitative PCR. *Nucleic acids research,* 39**,** e63-e63.

WALSH, A. L., CONSIDINE, S. W., THOMAS, A. Z., LYNCH, T. H. & MANECKSHA, R. P. 2014. Digital rectal examination in primary care is important for early detection of prostate cancer: a retrospective cohort analysis study. *British Journal of General Practice,* 64**,** e783-e787.

WARNICH, L., I DROGEMOLLER, B., S PEPPER, M., DANDARA, C. & EB WRIGHT, G. 2011. Pharmacogenomic research in South Africa: lessons learned and future opportunities in the rainbow nation. *Current Pharmacogenomics and Personalized Medicine (Formerly Current Pharmacogenomics),* 9**,** 191-207.

WESTON, R., COSTELLO, A. J. & MURPHY, D. G. 2012. Prostate Cancer Diagnosis. *In:* DASGUPTA, P. & KIRBY, R. S. (eds.) *ABC of Prostate Cancer.* 1st ed. UK: Blackwell Publishing Ltd, pp 11-12.

WILLIAM, R., WATSON, G. & FITZPATRICK, J. 2012. Biology of Prostate Cancer. *In:* DASGUPTA, P. & KIRBY, R. (eds.) *ABC of Prostate Cancer.* 1st ed. UK: Blackwell Publishing Ltd, pp 10.

YI, Q.-Q., YANG, R., SHI, J.-F., ZENG, N.-Y., LIANG, D.-Y., SHA, S. & CHANG, Q. 2020. Effect of preservation time of formalin-fixed paraffin-embedded tissues on extractable DNA and RNA quantity. *Journal of International Medical Research,* 48**,** 0300060520931259.

ZERBIB, M., ZELEFSKY, M. J., HIGANO, C. S. & CARROLL, P. R. 2008. Conventional treatments of localized prostate cancer. *Urology,* 72**,** S25-S35.

ZHENG, Z., ZHOU, Z., YAN, W., ZHOU, Y., CHEN, C., LI, H. & JI, Z. 2020. Tumor characteristics, treatments, and survival outcomes in prostate cancer patients with a PSA level< 4 ng/ml: a population-based study. *BMC cancer,* 20**,** 1-7.